Contribution of climate models and APSIM phenological parameters to uncertainties in spring wheat simulations: application of SUFI-2 algorithm in northeast Australia

Brian Collins [1*], Ullah Najeeb [1], Qunying Luo [2] and Daniel K.Y. Tan [3]

1. The University of Queensland, the Queensland Alliance for Agriculture and Food Innovation (QAAFI), Toowoomba, QLD 4350, Australia.

2. Hillridge Technology Pty Ltd, Sydney 2006, Australia.

3. Institute of Agriculture, School of Life and Environmental Sciences, Faculty of Science, The University of Sydney, Sydney, NSW 2006, Australia.

Abstract

We used SUFI-2 for the first time to calibrate the phenology module of the APSIM-wheat model for 10 spring wheat cultivars cultivated in northeast Australia (south-eastern Queensland). Calibration resulted in an average RMSE of 5.5 d for developmental stages from stem elongation up to flowering. Projections from 33 climate models under the representative concentration pathway 8.5 were used for simulations at 17 sites. Using adapted sowing times, we simulated significantly shorter crop cycles and grain yield improvements for the period 2036-2065 relative to 1990-2019 for three selected cultivars (Hartog, Scout and Gregory). Photoperiod and vernalisation sensitivities were shown to be the largest and smallest contributors to total uncertainties in the simulated flowering day and grain yield. Uncertainties in climate models had a relatively minor contribution to the total uncertainties in the simulated values of target traits. This contribution significantly increased when climate change impact on the target traits was estimated.

Keywords: Australian wheatbelt, calibration, climate change, crop model, sensitivity analysis, uncertainty analysis.

1   Introduction

Crop phenology, i.e. knowledge of crop developmental phases, is essential for precision farming and crop management. It is a key component of crop models that use cultivar-specific parameters to simulate growth, development and yield of a crop. There has been an increased application of process-based crop models to address the interactive impact of genotype × environment × management interactions (G×E×M) on crop yield and development under a changing climate (e.g. Zheng et al., 2012; Lobell et al., 2015; Stöckle et al., 2018; Webber et al., 2018; Hunt et al., 2019; Liu et al., 2019, 2020; Ababaei and Najeeb, 2020). Crop models have also been extensively adopted in climate change impact and adaptation studies across Australia (Yang et al., 2014; Luo et al., 2018; Hunt et al., 2019; Ababaei and Najeeb, 2020; Liu et al., 2020) and worldwide (Ababaei and Ramezani Etedali, 2017; Stöckle et al., 2018; Liu et al., 2019; Asseng et al., 2015; Challinor et al., 2009a; Pörtner et al., 2014; Rosenzweig et al., 2014). However, due to the complex nature of bio-physical factors associated with crop production processes, many uncertainties originate while simulating the impact of the future climate on crops. Sources of uncertainty include projection of greenhouse gas emissions, projection of global warming, projection of local climate change, estimation of crop model parameters and crop model structure (Zhang et al., 2019; White et al., 2011; Challinor et al., 2013; Wallach and Thorburn, 2017).

Previous studies quantified the effect of these uncertainties on estimates of climate change impact on crop production. For example, Luo et al. (2005) and Tao et al. (2008) used the Monte Carlo technique to quantify and manage uncertainties from climate change projections. Studies by Iizumi et al. (2009) and Zhang et al. (2019) used the Markov Chain Monte Carlo (MCMC) technique for examining the probability distribution of biophysical parameters. Asseng et al. (2013), Araya et al. (2015) and Wang et al. (2017) reported a greater contribution of crop model structure to the total uncertainty than general circulation models (GCMs). In contrast, greater uncertainties in crop yield projections from GCMs than those from crop model structure were reported by Tao et al. (2009), Kassie et al. (2015) and Zhang et al. (2019). These conflicting findings show the necessity of assessing each source of uncertainty with the target model(s), within the target study area, and for the target crop(s).

Among these sources, crop model parameter estimation (the so-called crop model calibration or inverse modelling) can be an important source of uncertainty. Calibration is a critical step in developing and applying a simulation model, which uses observational data to estimate unknown model parameters for a better fit of model outputs (Seidel et al., 2018). Common goodness-of-fit criteria for determining crop parameters include visual assessment and statistical/optimisation

58   approaches such as maximum likelihood, ordinary least square, D-statistics (Willmott, 1982), and

59   Bayesian analysis. Some calibration algorithms also generate useful statistical information such as

60   parameter sensitivities for supporting calibration. Compared to direct measurement of parameters

61   in the field, which is time and cost consuming, inverse modelling generates inferences from

62   common measured phenological and production components. Recently, there has been an

63   increased interest in using inverse modelling for calibrating crop models (e.g., Ababaei et al., 2014;

64   Andarzian et al., 2015; Yuan et al., 2017; Hussain et al., 2018; Zhang et al., 2019; Gao et al., 2020).

65   However, most of the previous studies explored the impact of uncertainties in model parameters

66   on the target outputs by assigning arbitrary ranges of variations to a number of parameters (e.g.

67   Bert et al., 2007; DeJonge et al., 2012; Zhao et al., 2014), usually based on literature or previous

68   experiences. This approach could lead to unrealistically large impacts on selected outputs as it does

69   not account for the uncertainty in observations and the interaction between the parameter

70   uncertainty and model structure uncertainty under local conditions.

71   Soil and crop models have a large array of biophysical and physiological parameters. For such

72   complex models, a sensitivity analysis helps to identify the importance of each parameter to the

73   response of target output variables (Richter et al., 2010). Sensitivity analysis has so far been applied

74   to different cropping systems and climate scenarios to evaluate the importance of input parameters

75   for target outputs using agro-hydrological models (Asseng et al., 2004; DeJonge et al., 2012; Kumar

76   et al., 2014; Zhao et al., 2014). Asseng et al. (2004) showed complex interactions between

77   phenological and physiological traits in high and low yielding environments for wheat yield. The

78   model outputs could be sensitive to both individual parameters and their combinations (Pogson

79   et al., 2012) and the sensitivities of parameters depend on model complexity, the number of crop

80   parameters included in the analysis and the environment (Richter et al., 2010).

81   Hence, the objectives of present study were to: (1) calibrate phenology module of the widely used

82   Agricultural Production Systems sIMulator (APSIM)-wheat model with a modified version of the

83   SUFI-2 (Sequential Uncertainty Fitting, ver. 2; Abbaspour et al., 2004) calibration and uncertainty

84   analysis algorithm, (2) examine sensitivities of the selected phenological parameters under current

85   and future climate scenarios, (3) assess the impact of parameter uncertainty on the simulated

86   phenology and grain yield and also on the quantification of the impact of climate change on these

87   traits, and (4) evaluate the impact of climate change on wheat crops in northeast Australia.

2   Materials and methods

2.1   Field experiments

Eight field experiments were conducted over 2 years (2018–2019) at three different locations across southern Queensland, Australia (Table 1). Randomised block design trials with two times of sowing (TOS) and four replicates were conducted each year. Zadoks growth stage (Zadoks et al., 1974) was recorded from stem elongation (Z31) up to flowering (Z65) for all genotypes. Phenology data were recorded as an average of the whole plot (i.e. at least 50% of culms in the plot). Wheat crops were planted late in the cropping season, to ensure they would receive high temperatures during different developmental phases. For example, the crop was planted on July 3 and 9 (conventional sowing) and August 31 and September 3 (late sowing) at The University of Queensland Research Farm, Gatton (27°34'50"S 152°19'28"E). The experiments were also conducted at the Hermitage Research Station, Warwick (28°12'40"S, 152°06'06"E) and Tosari Crop Research Centre, Tummaville (27°54'60"S, 151°30'0"E) with sowing on July 16 (conventional sowing), and September 12 and September 6 (late sowing) in 2018 and 2019, respectively. All the experiments were planted using a cone seeder with a target population of 100 plants m^{-2} and a row-spacing of 250 mm within 5 m × 1 m plots. The crops were irrigated at sowing and cultivated under non-limiting fertiliser conditions. Standard crop management practices including weed, disease and pest control were adopted.

Table 1. Field experiments used for calibrating the phenological parameters.

Location	Coordinates		Previous crop	Sowing dates		Year	Irrigation
	S	E					
University of Queensland Research Farm, Gatton	27° 34' 50"	152° 19' 28"	Fallow	03-Jul	31-Aug	2018	Full
				09-Jul	03-Sep	2019	Full
Hermitage Research Station, Warwick	28° 12' 40"	152° 06' 06"	Fallow	16-Jul	12-Sep	2018	Supplementary
Tosari Crop Research Centre, Tummaville	27° 54' 60"	151° 30' 0"	Cotton	16-Jul	06-Sep	2019	Supplementary

Ten commercial Australian bread wheat (*Triticum aestivum* L.) cultivars with contrasting phenology and adaptation were used in this study (Table 2). These include three high-performing spring cultivars with a wider adaptation to Australian environments i.e. Suntop (mid-season maturity), Mace (early to mid-season maturity) and Scout (mid-season maturity).

2.2   Calibration and uncertainty analysis algorithm

In this study, SUFI-2 calibration and uncertainty analysis algorithm was adopted for calibration of APSIM-wheat crop model (version 7.10). To the best of our knowledge, the present study is the first to use this algorithm for calibrating a crop model. The original SUFI-2 has been implemented

115 in SWAT Calibration and Uncertainty Programs (SWAT-CUP; Abbaspour et al., 2007a;

116 Abbaspour, 2015), which is designed for calibration of Soil and Water Assessment Tool (SWAT).

117 SUFI-2 accounts for the uncertainties in observations while estimating parameter values and

118 performs uncertainty analysis at the same time as parameter estimation. A modified version of

119 SUFI-2 (hereafter, 'SUFI-2M') was implemented in a customised package in the R programming

120 environment (R Core Team, 2017).

121 Table 2. List of the cultivars with varying maturity type and adaptation.

Cultivar	Maturity type	Adaptation	Reference
Suntop	Mid maturing	Widely adapted to Australian environments	Graham et al., 2015
Mace	Mid to slow maturing	Widely adapted to Australian environments	Graham et al., 2015
Scout	Mid maturing	Widely adapted to Australian environments	Graham et al., 2015
EGA Gregory	Mid to slow maturing	Nematodes resistance	Graham et al., 2015
EGA Wylie	Mid to slow maturing	Fusarium crown rot resistance	Zheng et al., 2014
Seri-82	Mid to slow maturing	Drought tolerance	Christopher et al., 2008
Drysdale	Mid to slow maturing	Drought tolerance	Condon et al., 2012; Tausz-Posch et al., 2012
Spitfire	Fast to mid maturing	High grain protein	Graham et al., 2015; Brill et al., 2013
Hartog	Fast to mid maturing	Drought susceptible	Brennan et al., 1991; Christopher et al., 2008
Janz	Fast to mid maturing	Straw strength and standability	Brennan et al., 1991

122 A step-by-step description of SUFI-2 has been presented by Abbaspour et al. (2007b). All steps

123 and related equations are presented in the Supplementary Material. Briefly, initial uncertainty

124 ranges are allocated to the selected parameters for the first round of sampling. These ranges are

125 subjective and are selected based on literature or previous experience. Then, a Latin Hypercube

126 (LH; McKay et al., 1979) sampling is carried out leading to LH_n (here, 200) parameter

127 combinations, which should be relatively large. The model is then run LH_n times and the target

128 traits are stored. A goal function (here, root mean square error, RMSE) is calculated and the

129 sensitivity matrix is created. Next, an equivalent of a Hessian matrix is calculated (Abbaspour et

130 al., 2007b). Then, an estimate of the lower bound of the parameter covariance matrix (C) is made

131 (Press et al., 1992) using variance of the objective function values resulting from the LHn runs.

132 The estimated standard deviation and 95% confidence interval of each parameter is calculated

133 from the diagonal elements of the covariance matrix. As all parameters are allowed to change, the

134 correlation between any two parameters is quite small and can be evaluated with the diagonal and

135 off-diagonal terms of C.

136 SUFI-2 calculates the 95% prediction uncertainties (95PPU) for all the variables in the objective

137 function (i.e. values of target traits). It is calculated by the 2.5th and 97.5th quantiles of the

138 cumulative distribution of simulated points. The aim is to encapsulate as many measured data as

139 possible within the 95PPU band (P-factor: percentage of observed data that fall within the 95PPU),

140   and to reduce average distance between the upper and the lower 95PPU (d-Factor: the degree of

141   uncertainty). The 'ideal' outcome is that 100% of the measurements fall within the 95PPU range

142   and d-Factor is close to zero (Abbaspour et al., 2007b). This ideal situation is generally not

143   achievable. We seek to see most of observations fall within the 95PPU range. At the same time,

144   we prefer to have a small 95PPU range (i.e. uncertainty range). No specific recommendation exists

145   for these two factors, like any other goodness of fit measure. However, a value of >70% can be

146   suggested for P-factor while having R-factor of around 1 is acceptable (Abbaspour et al., 2007b).

147   Parameter ranges are updated at the end of each iteration. This approach ensures that the updated

148   parameter ranges are always cantered around the best estimates. It is recommended that of the

149   highly correlated parameters, those with smaller sensitivities should be fixed to their best estimates

150   and removed from additional sampling rounds (Abbaspour et al., 2007b). For the present study,

151   number of iterations was set to 100.

152   A few modifications were introduced to the original SUFI-2 routine. First, updating parameter

153   ranges in SUFI-2M is performed at the beginning of each iteration instead of at the end. This way,

154   we assure that the finally selected 'best' parameter set has been chosen from a range of which the

155   corresponding 95PPU range brackets a pre-defined percentage of observations (here, 70%). If the

156   updating is performed at the end of each iteration, final parameter ranges may or may not satisfy

157   this criterion. In the modified version, parameter ranges are not updated if no improvement in the

158   goal function has been achieved. Moreover, only the best parameter set is used to update the

159   parameter ranges, instead of using the average of the top p (a user-defined number) best parameter

160   sets, which is the case in the original version.

161   Another modification was the introduction of a 'boosting' option. With this option, LH_n is reduced

162   at the beginning of each iteration (see Supplementary Material for the equations). This option

163   reduces LH_n proportionally to changes in parameter ranges and makes the optimisation procedure

164   significantly faster.

165   **2.3   Calibration setup**

166   Four phenological parameters were selected for calibration based on previous experiences on

167   model performance: (1) vernalisation sensitivity (vern_sens), (2) photoperiod sensitivity

168   (photop_sens), (3) thermal time from 'end of juvenile' to 'floral initiation' (tt_end_of_juvenile),

169   and (4) thermal time from 'floral initiation' to 'flowering' (tt_floral_initiation). To evaluate the

170   capability of SUFI-2M for crop model calibration, the selected phenological parameters were

171   calibrated for 10 selected spring wheat cultivars. Following a common and widely accepted

172 approach (e.g. Chenu et al., 2011; Hammer et al., 2014; Lobell et al., 2015; Zheng et al., 2016; An-

173 Vo et al., 2018; Ababaei et al., 2019), most crop parameters were assumed to be similar across

174 cultivars and therefore equal to the default values for the base cultivar (i.e. Hartog). Observed

175 phenology data from Gatton 2018 (second sowing) and Gatton 2019 (first sowing) experiments

176 were used for validation (i.e. ~35% of the observations) each representative of a number of trials

177 in terms of heat-shock and drought patterns. The rest of the data were used for calibration. In

178 order to consider the uncertainty in observations and account for its impact on parameter

179 estimation, all replications were used for calibration as independent measurements.

2.4 Simulation setup

181 The APSIM-wheat model (Keating et al., 2003; Holzworth et al., 2014), which has been widely

182 tested and used in Australia (e.g. Asseng et al., 2001; Lilley and Kirkegaard, 2007; Hochman et al.,

183 2009; Chenu et al., 2011; Christopher et al., 2016; Wang et al., 2018; Ababaei and Chenu, 2019,

184 2020; Ababaei and Najeeb, 2020), was adopted (version 7.10) to simulate wheat crop growth and

185 development under current and future climate scenarios. Heat-shock and frost impacts were

186 estimated using methods described by Lobell et al. (2015), Ababaei and Chenu (2020) and Zheng

187 et al. (2015a).

188 Out of ten calibrated spring wheat cultivars, three cultivars (Hartog, Scout and Gregory) of

189 contrasting maturity habits and different ranges of parameter uncertainties were chosen for

190 simulations with sowing dates between April 1 and July 31 at 7-day intervals. At each location, soil

191 characteristics, initial soil nitrogen, fertilisation levels and planting density were set to represent

192 local soils and farming practices. (see Table 1 in Chenu et al., 2013). Soil initial conditions were

193 reset on January 1 each year to the median level based on long-term simulations (Chenu et al.,

194 2013). A small amount of irrigation was applied at sowing, if needed, to raise soil moisture of the

195 top layer to the lower limit of plant-extractable soil water so that seeds could germinate the day

196 after sowing.

2.5 Climate data

198 Historical daily weather data, including maximum and minimum temperature, solar radiation and

199 rainfall, were obtained from the SILO patched point dataset (http://apsrunet.apsim.info/cgi-

200 bin/silo; Jeffrey et al., 2001) for the period 1976-2019 at 17 selected sites across northeast Australia

201 (Figure 1; Ababaei and Chenu, 2020). Locations were selected to represent the wheat-producing

202 regions of Queensland and New South Wales (Chenu et al., 2013). Monthly projections of

203 precipitation and minimum and maximum temperatures from 33 GCMs for future period centred

204   on 2050 were obtained from the Coupled Model Intercomparison Project 5 (CIMIP5; Taylor et

205   al., 2012). Future climate scenarios were constructed for 2036-2065 (hereafter, the '2050' climate)

206   by downscaling to a daily time step. Downscaling was performed by applying projected changes in

207   local monthly means to the daily temperature and rainfall data for the period of 1976-2005 (Lobell

208   et al., 2015). The 30-year period of 1990-2019 (hereafter, the '2005' climate) was simulated as the

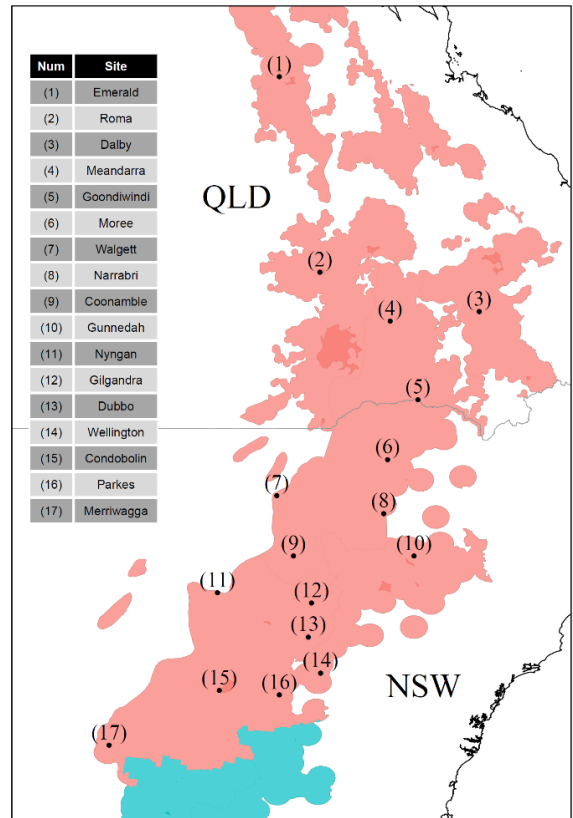209   benchmark scenario to quantify the impact of climate change.

210

211   Figure 1. The 17 selected sites representative of the major wheat-producing regions in northeast Australia

212   (depicted with red shading).

213   Atmospheric [CO_2] was set at 541 ppm for the 2050 climate, as projected by the representative

214   concentration pathway (RCP) 8.5, which assumes 'business as usual' CO_2 emission. For the 2005

215   climate, atmospheric [CO_2] data was obtained from Ziehn et al. (2016). In APSIM-wheat, elevated

216   [CO_2] linearly increases transpiration efficiency from a cultivar-specific reference value at 350 ppm

217   by 37% when [CO_2] reaches 700 ppm (Reyenga et al., 1999). It is also related to the radiation use

218   efficiency (RUE) which is adjusted with a temperature response function. In APSIM-wheat, RUE

219   at 20°C increases by 14% when [CO_2] increases to 541 ppm (Lobell et al., 2015).

8

2.6 Optimum sowing dates

The 'best' sowing date in each season, i.e. leading to the highest grain yield, was used to quantify the target traits (flowering date and grain yield) under each climate scenario. This was done to minimise the effect of suboptimal management choices and give a more realistic evaluation of the 'net' impact of climate change on wheat crops when cultivated on the best sowing date in each season. In order to investigate the impact of climate change on optimum sowing dates, sowing windows were determined separately under each climate scenario. For the 2050 climate, one common sowing window was identified for all the GCMs. The windows were determined as the period between 25th and 75th quantiles of the selected dates over the 30 simulated seasons.

2.7 Quantifying the impact of parameter uncertainty on simulated traits

Any uncertainty in estimated values of crop parameters may lead to substantial deviations in the simulated values of target traits from the values simulated by the 'best' calibrated parameter sets. Therefore, after calibration was performed and the final parameter ranges were determined for each cultivar, a set of parameter values (hereafter, 'uncertain' parameter sets) was created for each cultivar to analyse the impact of parameter uncertainties on the simulated values of the target traits (flowering day and grain yield). To that end, the lower and upper bounds and the mid-point of each parameter range were chosen. Each combination of these three values and the four selected parameters ($3^4 = 81$ parameter sets) was considered as an individual 'virtual' cultivar. For each parameter, the 'uncertain' parameter sets represent the range of uncertainty around the 'best' parameter value and allow quantification of the impact of uncertainties on the simulated traits.

We evaluated the contributions of model parameters and climate models to the total uncertainty of target traits using an Analysis of Variance (ANOVA; Tao et al., 2018; Zhang et al., 2019). Variance components were estimated as the corresponding contribution (in percentage) of each factor to the total sum of squares. 'Cultivar uncertainty' was estimated as the variation of target traits across the 'virtual' cultivars while the simulated target traits were averaged across the GCMs. 'GCM uncertainty' was estimated as the variation of target traits across the 33 GCMs while averaged across the 'virtual' cultivars.

2.8 Sensitivity analysis of APSIM-wheat phenological parameters

APSIM-wheat sensitivities to uncertainties in wheat phenological parameters were evaluated with a global sensitivity analysis (GSA) approach (Abbaspour et al., 2007b; Faramarzi et al., 2010; Abbaspour, 2015). GSA overcomes the drawbacks of local optima (or one-at-a-time) approaches

9

251   by exploring the entire multi-dimensional parameter space simultaneously, leading to a better

252   quantification of the influence of each parameter and the interactions between parameters (Saltelli

253   et al., 2008). A multiple linear regression system, which relates the parameters generated by the

254   Latin Hypercube sampling to the objective function values (i.e. the values of target traits) in all

255   simulated seasons, was separately constructed for each season as well as for all simulated seasons

256   together. A t-test was used to identify the significance of each estimated parameter value. The

257   sensitivity indices (SI) calculated by this method are estimates of the average changes in the target

258   traits (here, flowering day and grain yield) stemming from uncertainties in each parameter while all

259   other parameters are also changing. That is, the SIs are based on linear approximations and only

260   provide partial information about the sensitivity of the objective function to model parameters.

261   Sensitivity analysis was independently performed under the 2005 and 2050 climates. To quantify

262   the contribution of climate models to the total uncertainty in parameter sensitivities, sensitivity

263   analysis was performed for each GCM separately as well as for all GCMs collectively under the

264   2050 climate. As the range of selected parameters were different, each parameter was scaled (by

265   subtracting the average and dividing by the standard deviation) before fitting the multiple linear

266   regressions. To obtain a better understanding of the magnitude of sensitivities, we further

267   compared the contributions of location, climate models and inter-annual variability to the total

268   variance of target traits using ANOVA.

3   Results

3.1   Parameter calibration

271   Calibration was performed with the aim of encapsulating at least 70% of the observed phenology

272   data within the uncertainty range of model simulations (95PPU). Figure 2 shows the observed vs

273   simulated phenology for the 10 wheat cultivars calibrated with SUFI-2M along with the simulation

274   uncertainty ranges. The overall root mean square error (RMSE) of the calibration/validation phase

275   was 5.6/5.5 d (Figure 2). Calibration significantly improved model performance compared with

276   when the APSIM default parameters were adopted (Supplementary Material Figure S1).

277   Considering all the individual replications, the lowest and highest errors were related to *cv* Hartog

278   (RMSE = 3.9 d; Figure 3a), and *cv* Seri-82 and Drysdale (RMSE = 7.1 d), respectively. Figure 3b

279   presents the 'best' calibrated value for phenological parameters along with the uncertainty ranges
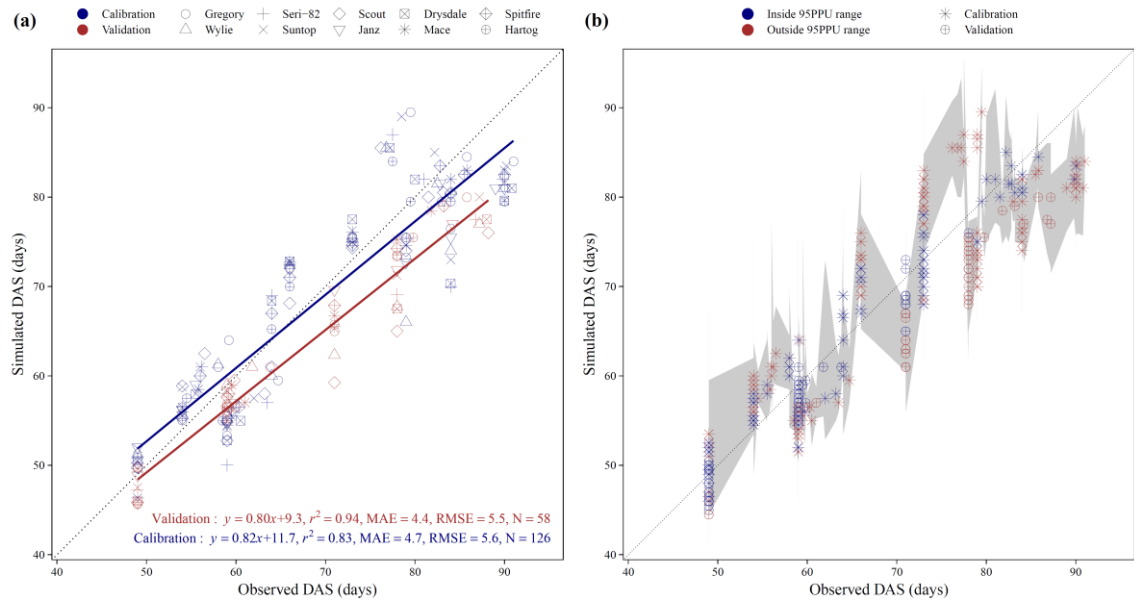
280   of the parameters.

281

Figure 2. APSIM-wheat calibration results with the SUFI-2M algorithm across three locations in northeast Australia (south-eastern Queensland): **(a)** calibration for the 10 selected spring wheat cultivars; **(b)** uncertainty ranges in the simulated phenology along with the observed phenology for all the individidual replications. Data were averaged across replications in panel **(a)**. RMSE is the root mean square error, MAE is the mean absolute error and N is the number of data points. Observations included Zadoks growth stages from stem elongation (Z31) up to flowering (Z65). 'Inside' and 'outside' refer to the 95% prediction uncertainties (95PPU) range and whether the observed values fell within this range or not.
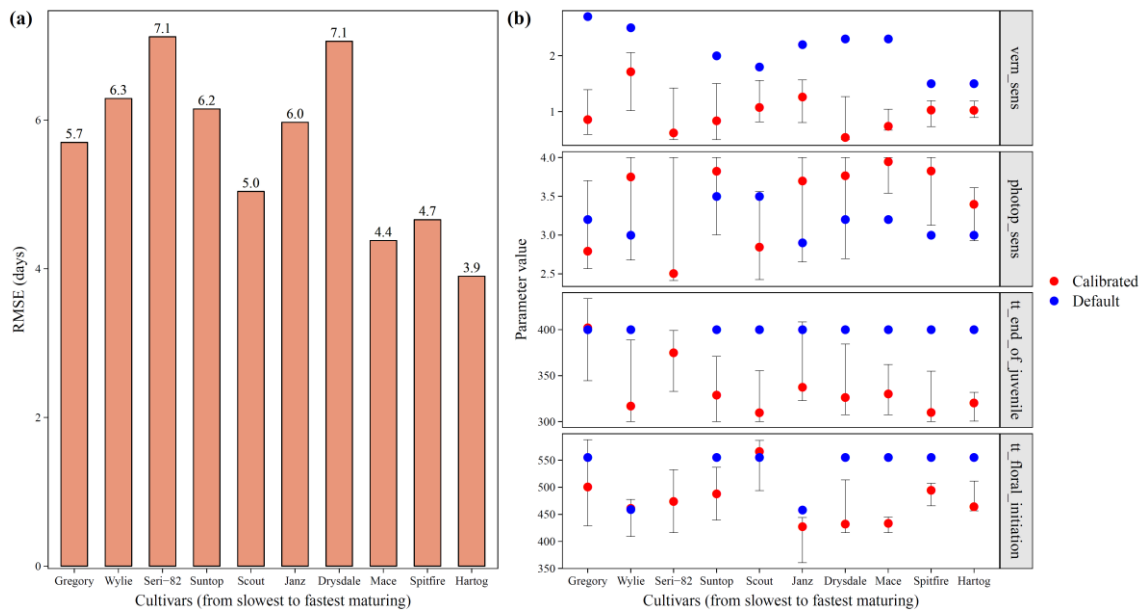
289

Figure 3. Root mean square error (RMSE) for the 10 selected spring wheat cultivars after calibration, considering all the individual replications **(a)**, and the 'best' calibrated values (red points) and uncertainty ranges (error bars) of each phenological parameter along with the default values of APSIM cultivar-specific parameters (blue points) **(b)**. Parameters included: (1) vernalisation sensitivity (vern_sens), (2) photoperiod sensitivity (photop_sens), (3) thermal time from 'end of juvenile' to 'floral initiation' (tt_end_of_juvenile), and (4) thermal time from 'floral initiation' to 'flowering' (tt_floral_initiation).

296

11

3.2 Climate change is expected to shift sowing dates to earlier dates in the season

Sowing windows were determined under each climate scenario separately for three spring wheat cultivars (Hartog, Scout and Gregory) of contrasting maturity habits (Figure S2). Under the 2050 climate and all the studied sites, except Emerald (for all cultivars) and Nyngan (only for *cv* Hartog), the start and mid-point of the sowing windows are expected to occur earlier in the season than in 2005. The shift was estimated to be 6.7, 7.0 and 7.9 d for the start date and 9.0, 9.8 and 11.9 d for the mid-point for Hartog, Scout and Gregory, respectively. Moreover, the sowing windows would be 7.5, 6.4 and 6.7 d shorter than those in 2005.

3.3 Crop model sensitivity changes over time and in space

Sensitivity of APSIM-wheat to uncertainties in crop phenological parameters varied over time (Figure 4; Supplementary Material Figures S3-S4) and in space (Supplementary Material Figure S5). For example for *cv* Hartog, approximately >92% of the total variance in the sensitivities of simulated flowering day and grain yield to changes in vernalisation sensitivity (vern_sens) was explained by residuals (i.e. inter-annual variations), which implies a high temporal variability in the SIs (Figure 5). These variance components were estimated to be larger in 2050 than in 2005, and for flowering day than for grain yield. Other parameters were more variable across the sites though the variance components were generally smaller in 2050 than in 2005 and larger for grain yield than for flowering day. Contribution of climate models to the total variance of the SIs was markedly smaller (<1%) than other sources of variance. On the other hand, 9-33% of the total variance in the sensitivity of flowering day to uncertainties in phenological parameters in 2050 was explained by location, while this component was generally smaller for grain yield.

3.4 Crop parameter sensitivities are expected to change in the future

For the four phenological parameters, we calculated the SIs related to wheat flowering day and grain yield under both climate scenarios (Figure 4). Among the calibrated parameters, uncertainties in photoperiod sensitivity ('photop_sens') was the most influential source of uncertainty on the simulated flowering day (Figure 4a), while vernalisation sensitivity ('vern_sens') was the least influential. Gregory, a slow-maturing spring cultivar, was most sensitive to uncertainties in 'photop_sens', 'tt_end_of_juvenile' and 'tt_floral_initiation' among the studied cultivars. These sensitivities are expected to slightly increase under future climate scenario, especially for 'photop_sens'.
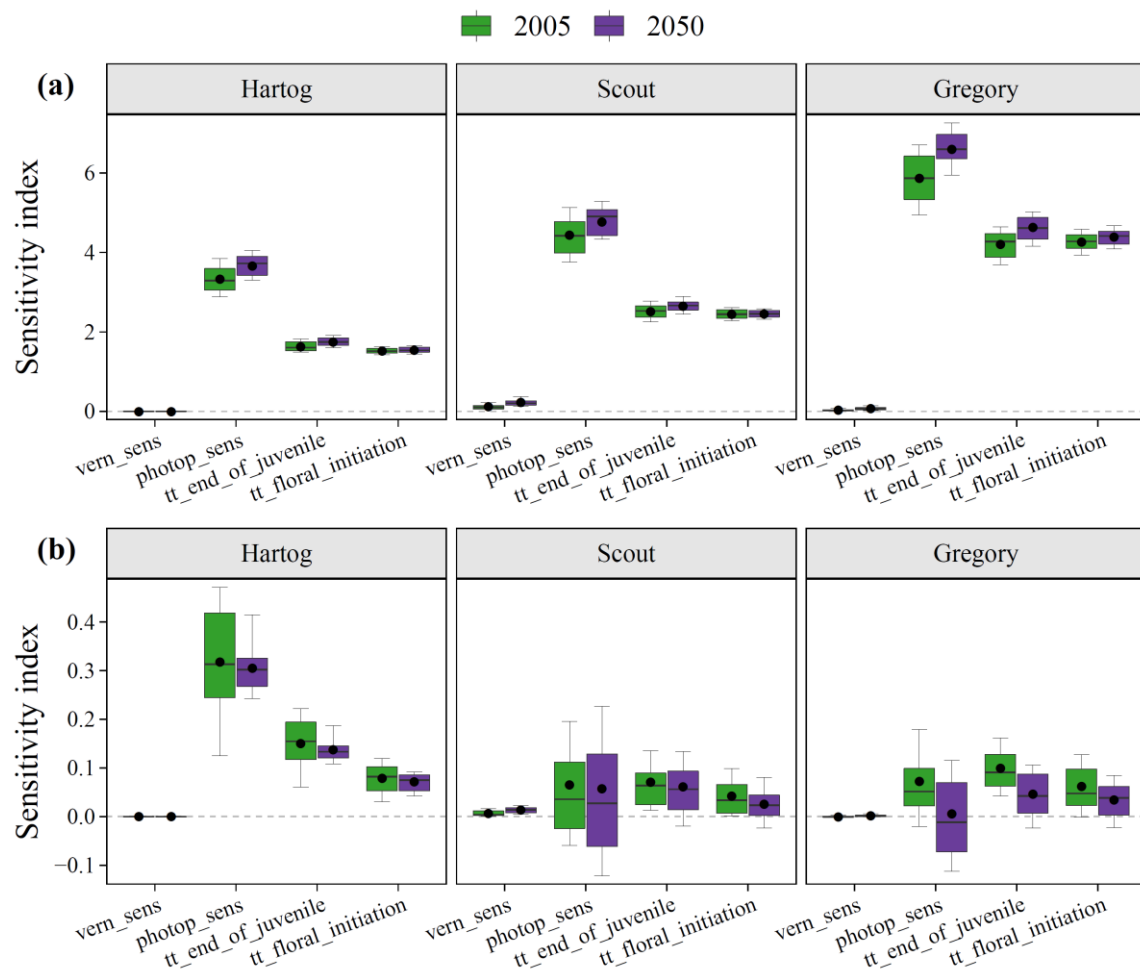
Figure 4. Sensitivity indices (SIs, averaged across 30 seasons) of the selected four phenological parameters for flowering day **(a)** and grain yield **(b)** under the 2005 (current) and 2050 (future) climates for three selected spring wheat cultivars across 17 sites in easutern Australia. Box plots show 10, 25, 50, 75 and 90th quantiles along with the means (black points). Parameters included: (1) vernalisation sensitivity (vern_sens), (2) photoperiod sensitivity (photop_sens), (3) thermal time from 'end of juvenile' to 'floral initiation' (tt_end_of_juvenile), and (4) thermal time from 'floral initiation' to 'flowering' (tt_floral_initiation).

The order of most sensitive parameters for grain yield was the same as for phenology (Figure 4b) for Hartog, however, the SIs were less variable across the selected sites for Scout and Gregory, except for 'vern_sens'. Unlike for flowering day, it is expected that the sensitivity of phenological parameters decreases in 2050 relative to 2005, though the shifts were generally insignificant for Hartog and Scout.

The only non-significant ($P>0.05$; i.e. P value of the t-test) SIs were related to 'vern_sens' for flowering day and across a few of the sites (Roma, Dalby, Meandarra and Walgett) for grain yield (Supplementary Material Figure S5). Sensitivity of flowering day to uncertainties in all the four parameters, except for 'vern_sens', generally increased from north to south (in the southern hemisphere) and the trend was strongest for 'photop_sens' under both climate scenarios. A similar

344 but relatively weaker trend was observed for grain yield, though the spatial patterns were more
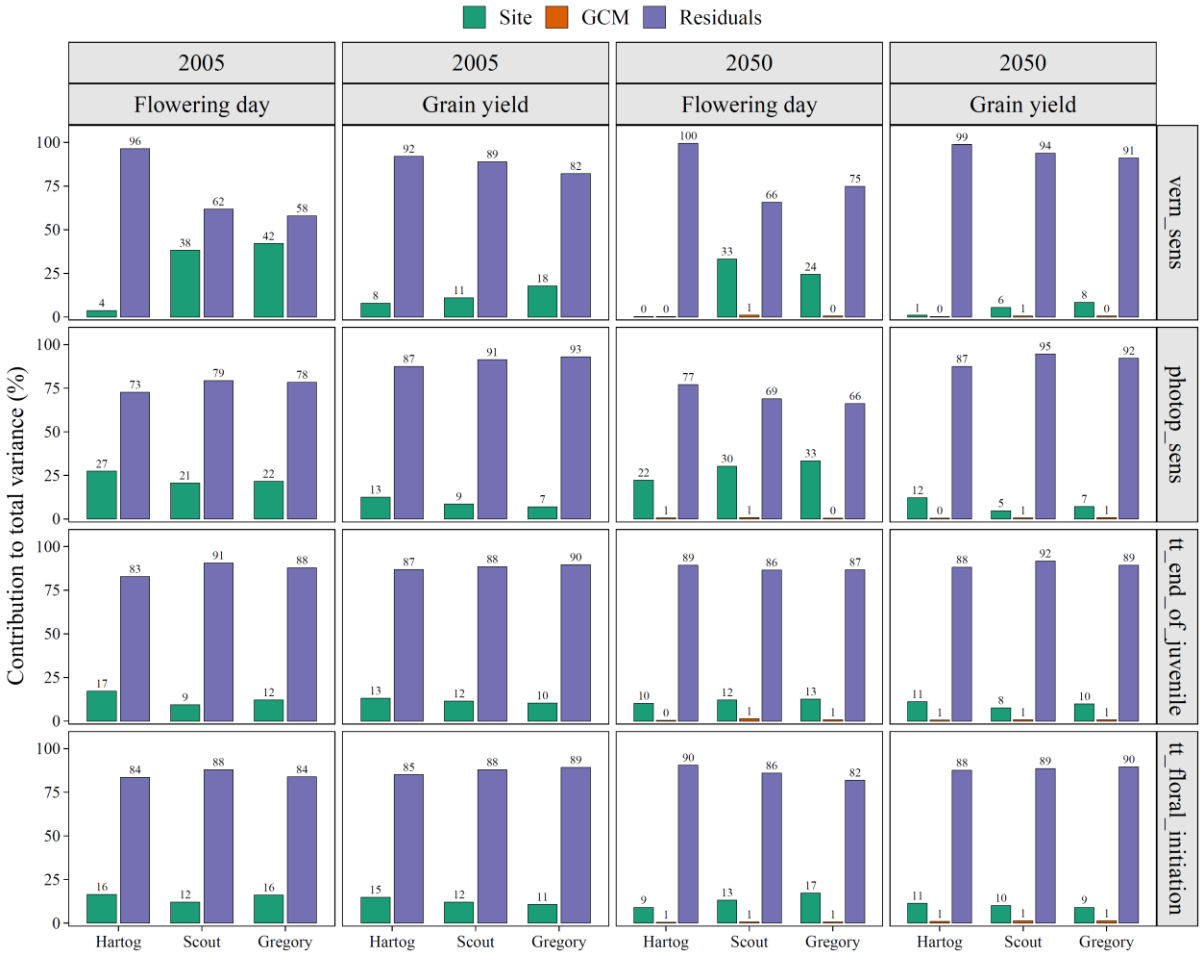
345 heterogeneous.

Figure 5. Variance components of the sensitivity of the target traits (flowering day and grain yield) to the four phenological parameters under the 2005 (current) and 2050 (future) climates for three selected spring wheat cultivars. Parameters included: (1) vernalisation sensitivity (vern_sens), (2) photoperiod sensitivity (photop_sens), (3) thermal time from 'end of juvenile' to 'floral initiation' (tt_end_of_juvenile), and (4) thermal time from 'floral initiation' to 'flowering' (tt_floral_initiation).

3.5 Parameter uncertainties affect trait quantifications

353 Larger uncertainties in phenological parameters of *cv* Scout and Gregory, as compared with Hartog,

354 led to larger deviations of simulated flowering day with uncertain parameter sets from the values

355 simulated with the 'best' parameter sets (Figure 6a), suggesting larger sensitivities. The mean

356 absolute errors (MAE) were estimated to be <1 d for Hartog under both climates and 3.9 and 4 d

357 for Gregory under the 2005 and 2050 climates, respectively. However, these deviations were not

358 directly reflected in the simulated grain yields (Figure 6b). While the uncertainty ranges for

359 phenological parameters were larger for Scout than for Hartog, the simulations with uncertain

360 parameter sets (representative of parameter uncertainties) resulted in smaller deviations from the

14

361   simulations with the 'best' parameter set (a normalized MAE of 11% for Scout vs 15% for Hartog

362   in 2005). This suggests that the simulated grain yield is more sensitive to other environmental and

363   management factors than flowering day is.
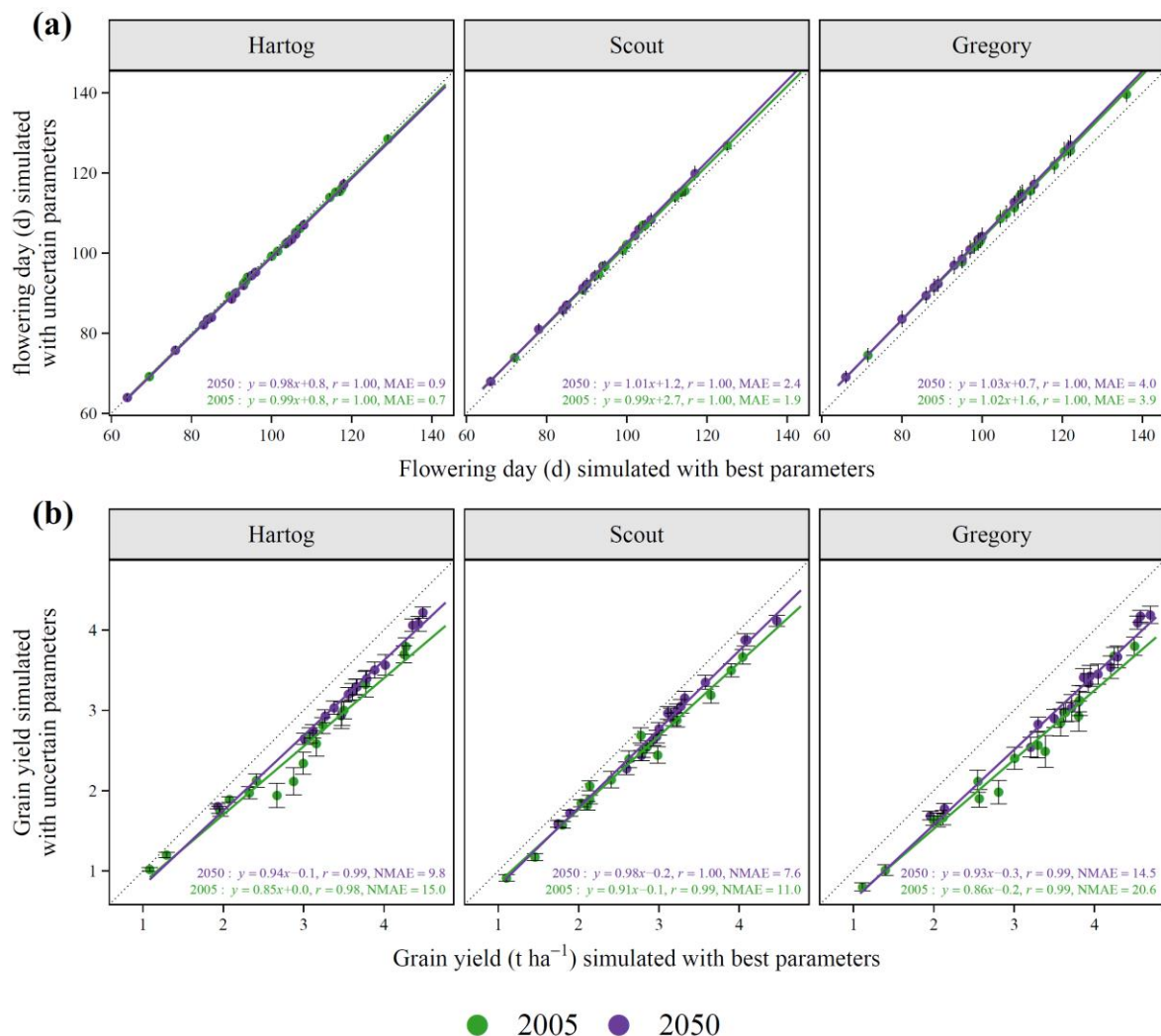

Figure 6. Flowering day **(a)** and grain yield **(b)**, averaged across 30 seasons, simulated with the best (x-axis) and uncertain (y-axis) parameter sets (averaged across 81 parameter combinations) for three selected spring wheat cultivars under the 2005 (current) and 2050 (future) climate scenarios. A larger deviation of y-axis values from x-axis values suggests a larger sensitivity.

3.6   Climate change is expected to enhance phenology and improve grain yield in northeast Australia

371   Wheat crops under the warmer and drier climate of 2050 were projected to reach flowering

372   significantly earlier as compared with 2005 (Figure 7a). Using the best (|uncertain) parameter sets

373   for three selected cultivars and at a regional scale, it was shown that Hartog, Scout and Gregory

374   would reach flowering day 9.9 (|10.2), 9.5 (|9.1) and 11.6 (|11.1) d earlier in 2050 than in 2005.

375   While this impact may reduce the time available for biomass assimilation, the wheat grain yield

15

376   could still benefit from the elevated atmospheric [CO_2] levels, leading to grain yield increases by

377   22.8 (|30.1), 20.4 (|24.3) and 25.1 (|32.5)% for the studied cultivars planted on the optimum

378   sowing dates (Figure 7b, Supplementary Material Figure S6). The results showed that the inclusion

379   of parameter uncertainties led to statistically significant deviations from the trait values simulated

380   with the 'best' parameter sets ($P<0.05$) for all the tested cultivars.
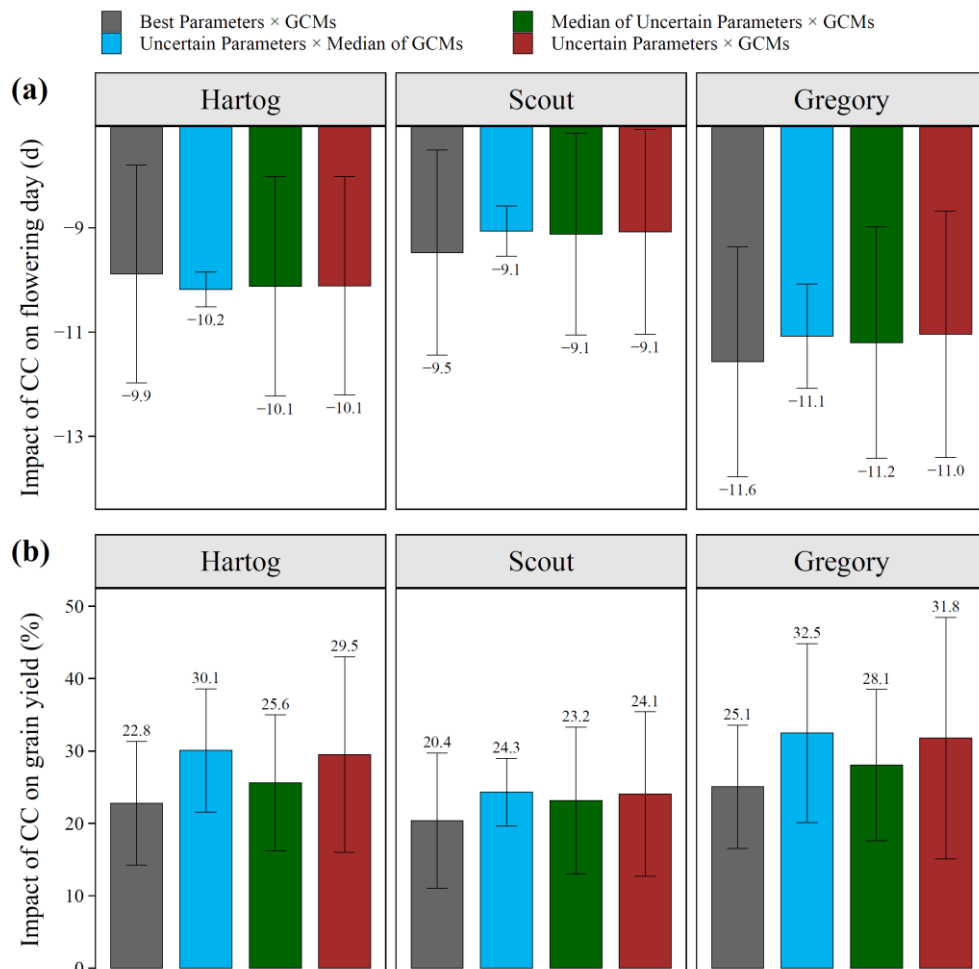

381

382   Figure 7. The impact of climate change (CC) on flowering day **(a)** and grain yield **(b)** at regional scale (i.e.
383   averaged acorss 30 seasons and 17 sites) simulated with the best and uncertain parameter sets for three
384   selected speing wheat cultivars. Error bars show standard deviation of the simulations across 33 GCMs
385   (gray, green and red bars) and 81 uncertain parameter sets (blue and red bars).

386   With the best sowing time adopted in each season under each climate scenario, it is anticipated

387   that all the studied cultivars would experience a significant improvement in grain yield level in 2050

388   relative to 2005 (Supplementary Material Figure S6), except in Emerald. Across all other locations,

389   it would be expected that Hartog, Scout and Gregory have higher grain yields by 9.7-63.1%, 5.4-

390   53% and 9.9-67.5%, respectively. Emerald was the only site that is expected to experience a

391   reduction in average grain yield in 2050, at which Hartog, Scout and Gregory were expected to

392   have lower simulated grain yields by 1.4, 2.8 and 2.5%, respectively.

393   Considering all the site × GCM combinations (Figure 8), 99.6, 99.4 and 99.9% of combinations

394   showed a negative shift in flowering day in 2050 for Hartog, Scout and Gregory, respectively. For

395   grain yield, in 95.5, 93.3 and 94.6% of the combinations a positive impact of climate change was

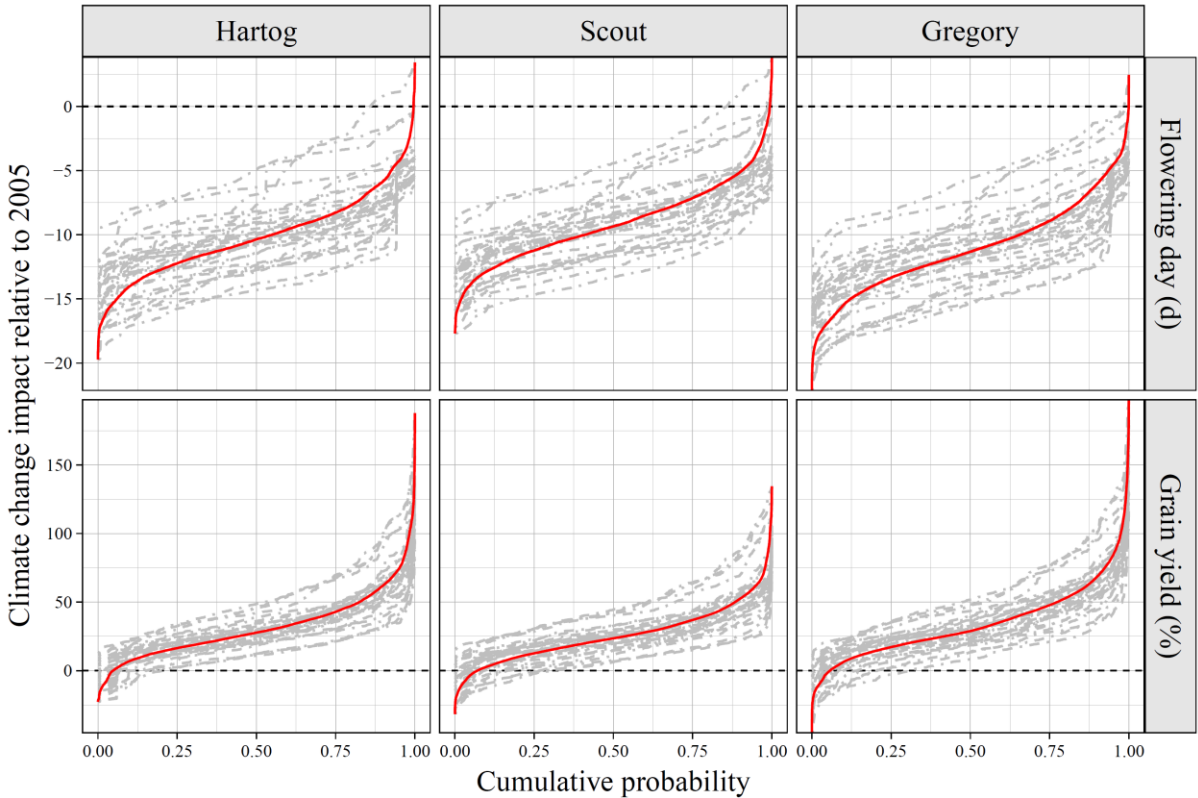396   simulated for the three cultivars.

397

398   Figure 8. The cumulative probability of the simulated impact of climate change on flowering day (absolute
399   change, d) and grain yield (relative change, %) with each of the 33 GMCs (gray lines) and all the GCMs
400   combined (red line) for three selected speing wheat cultivars. Cumulative probabilities on the horizontal
401   axis show the probability of observing impacts less than the numbers on the vertical axis.

402   **3.7   Contribution of crop parameters and climate models to simulation uncertainties**

403   Both crop parameters and climate models (GCMs) contribute to the uncertainties in the target

404   traits. Regarding absolute values of the target traits under the 2050 climate, the contribution of

405   crop parameters to uncertainties was larger than climate models (upper panels in Figure 9; Figure

406   10) while residuals (i.e. inter-annual variability) were the largest variance component. The

407   contribution of crop parameters to the total uncertainties in the simulated flowering day was larger

408   for Gregory and Scout than for Hartog, while this component was the smallest for grain yield of

409   Scout. The contribution of phenological parameters (|climate models) to the total uncertainties

410   were estimated to be 26 (|9), 38 (|7) and 55 (|5)% for the simulated flowering day and 15 (|8),10

411   (|8) and 16 (|7)% for the simulated grain yield for Hartog, Scout and Gregory, respectively.

17

412   On the other hand, the contribution of climate models to the total uncertainties in the simulated

413   impact of climate change (i.e. change in target traits in 2050 relative to 2005) on flowering day and

414   grain yield was significantly larger than crop parameters, especially for flowering day (lower panels

415   in Figure 9; Figure 10). Gregory (with the widest parameter uncertainty ranges) and Hartog (with

416   the narrowest parameter uncertainty ranges) had the lowest and highest contributions of

417   phenological parameter to the total variances, respectively.
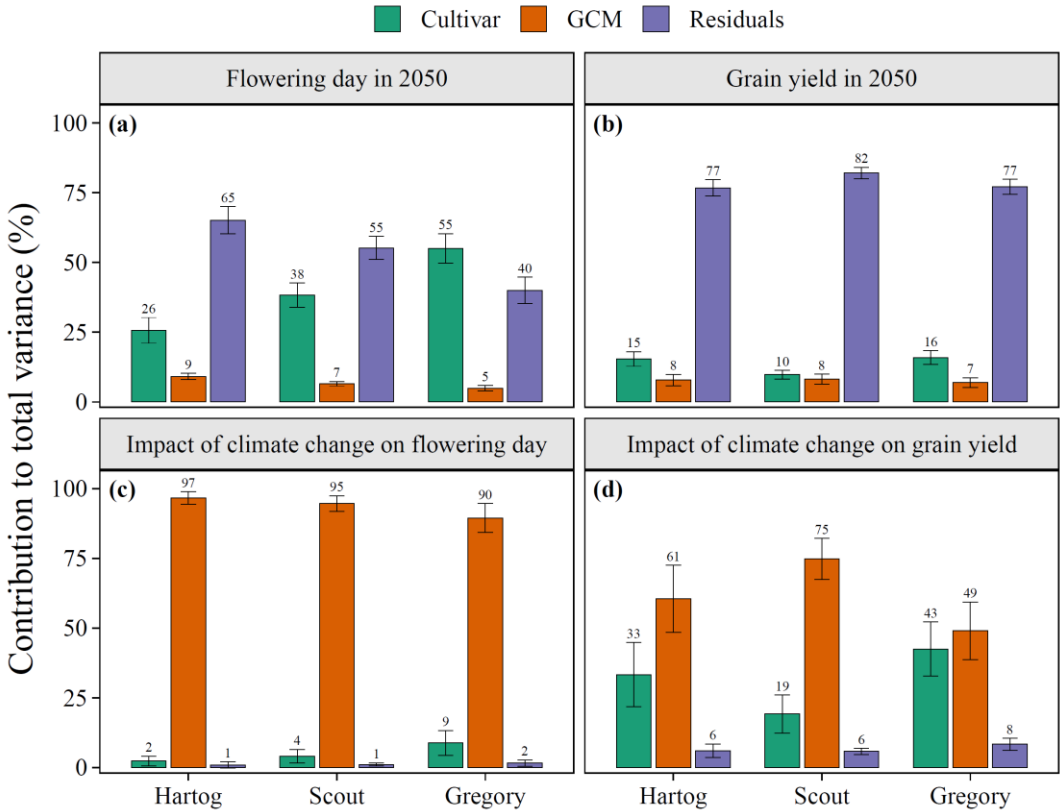

418

419   Figure 9. Variance components of the simulated values of the target traits (flowering day and grain yield)
420   under the 2050 climate **(a-b)** and of the simulated impact of climate change on each trait **(c-d)** for the three
421   selected cultivars. Values were averaged across the 17 selected sites in northeast Australia.

3.8   Spatial pattern of sensitivity indices in northeast Australia

423   Contributions of the two major sources of uncertainty to the total uncertainty in simulated

424   flowering day and grain yield and the impact of climate change on target traits were significantly

425   correlated with latitude (Figure 10). Considering all three cultivars, the correlation coefficient was

426   estimated to be -0.21 and 0.24 for flowering day, -0.41 and 0.51 for grain yield, -0.24 and 0.27 for

427   the impact of climate change on flowering day and -0.45 and -0.51 for the impact on grain yield,
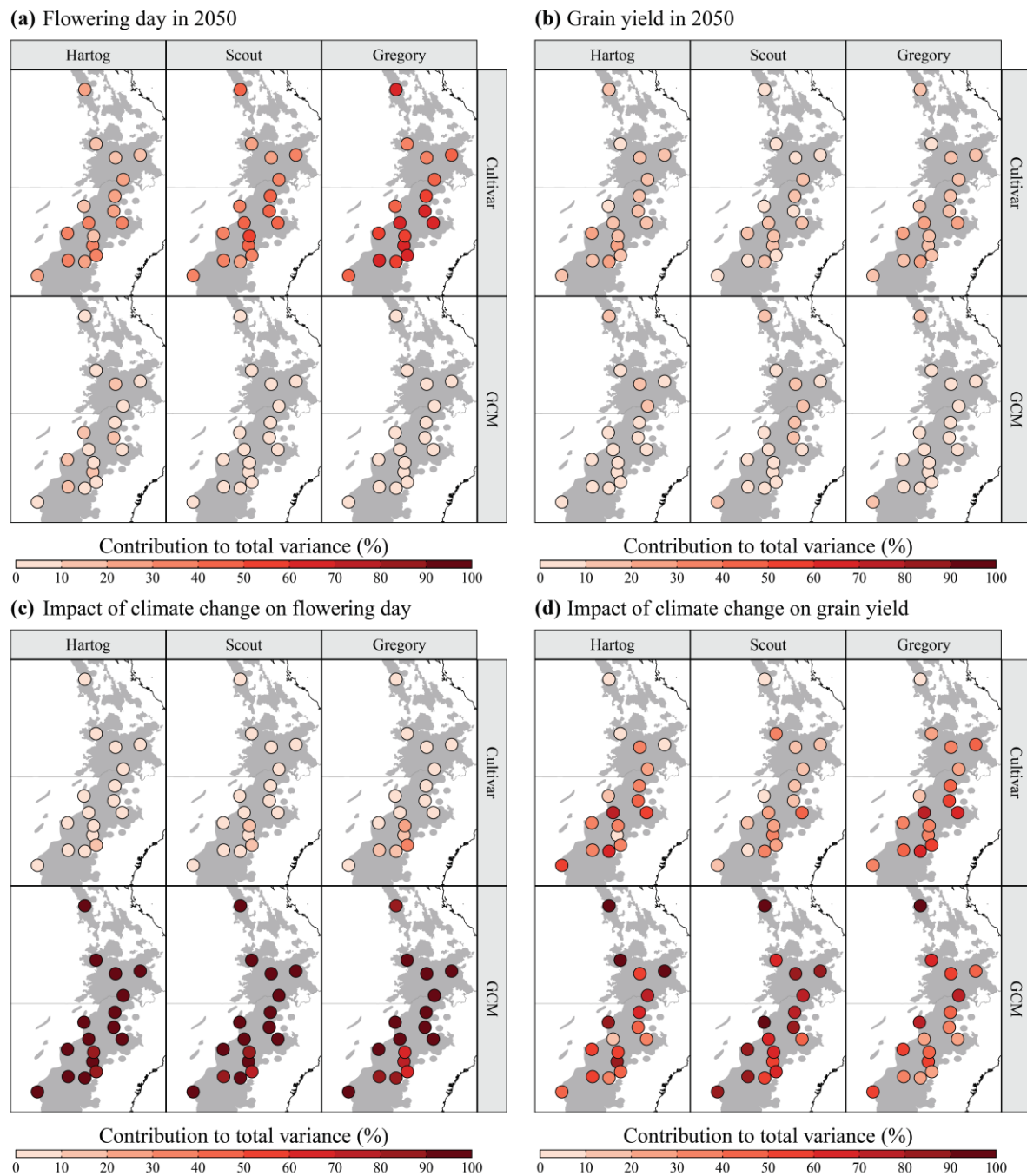
428   respectively.

Figure 10. Variance components of the simulated values of the target traits (flowering day and grain yield) under the 2050 climate **(a-b)** and of the simulated impact of climate change on each trait **(c-d)** for the three selected spring wheat cultivars across 17 selected sites in northeast Australia.

Figure 11 shows the impact of climate change on flowering day and grain yield simulated using the 'best' parameter sets against the averages of the simulations with the uncertain parameter sets. Considering all the uncertainties in the selected parameters, the impact of climate change on flowering day was simulated with a MAE of 0.2, 0.5 and 0.6 d for Hartog, Scout and Gregory, respectively. These deviations were smaller than the deviations estimated for the absolute values of the target traits under each climate scenario (Figure 6). The same was the case for grain yield,

439   with MAE values estimated to be 7, 4.3 and 7.6%. This implies that APSIM-wheat is more sensitive

440   to uncertainties in phenological parameters than uncertainties in climate models when the aim is

441   to quantify the absolute values of target traits under a future climate scenario. On the contrary, the

442   model is more sensitive to uncertainties in climate models when the target is to 'compare' the target

443   traits under current and future climate scenarios.

444
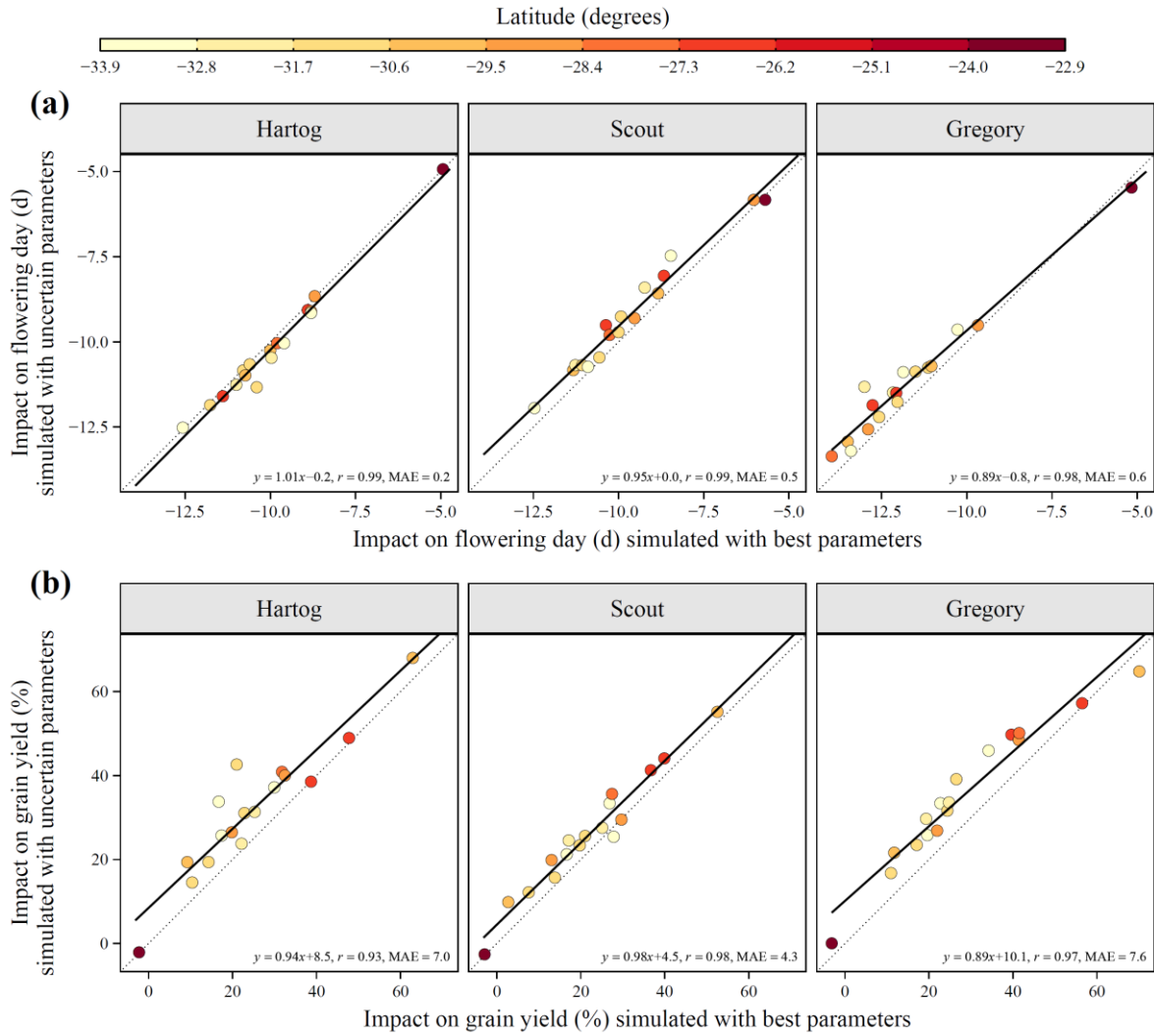
445   Figure 11. The impact of climate change on flowering day **(a)** and grain yield **(b)** of three selected spring
446   wheat cultivars. Values are averaged across 30 seasons, simulated with the best (x-axis) and uncertain (y-
447   axis) parameter sets (averaged across 81 parameter combinations). A larger deviation suggests a larger
448   sensitivity.

449   4   Discussion

450   4.1   Calibration

451   We successfully calibrated the APSIM-wheat crop model in northeast Australia (south-eastern

452   Queensland) using SUFI-2M algorithm. SUFI-2M resulted in a robust calibration of the model

453   with an overall RMSE of 5.5 d (3.9-7.1d) despite a considerable variations in the observed

454   phenology of the 10 selected wheat cultivars. While more detailed data on wheat growth stages

455   were used in this study than just data on heading, flowering or maturity days, these deviations are

456   considerably lower or at least comparable to the reported deviations by other similar studies, for

457   example, the reported RMSE for *cv* Janz was 6.2 d   for days to heading (Zheng et al. 2012) , 6.2 d

458   for flowering day (Flohr et al. 2017) , 7-8 d for flowering and maturity days of spring wheat cultivars

459   (Liu et al. 2018), 1.4–7.2 days for days to heading in barley (Liu et al. 2020) and 9.4-35.3 d for days

460   to flowering in rice (Gao et al. 2020).

461   In previous studies, other parameter estimation routines have been used for calibrating

462   hydrological and crop models. For example, Gao et al. (2020) applied three commonly used

463   calibration methods to the CSM-CERES-Rice phenology model of the Decision Support System

464   for Agrotechnology Transfer (DSSAT), including Ordinary Least Square (OLS), MCMC, and

465   Generalized Likelihood Uncertainty Estimation (GLUE). They reported that selection of the

466   calibration routine had implications for parameter estimates and uncertainty quantifications and

467   found MCMC more reliable than GLUE in quantifying model uncertainty. Iizumi et al. (2009) and

468   Tao et al. (2009) applied the MCMC technique to crop models for paddy rice and spring maize to

469   optimize a set of regional-specific parameters and quantified the uncertainty of yield estimation

470   associated with model parameters. They found that MCMC is a powerful technique to optimize

471   multiple parameters, to quantify their uncertainties and to investigate the impacts of climate

472   variability on crop productivity. As each of these techniques have been used with different crop

473   or hydrological models, in different locations and for different purposes/crops, it is not practically

474   possible to make a thorough comparison. Therefore, a choice should be made based on availability

475   of statistical knowledge, computation power and the objectives of the study.

476   **4.2   Sensitivity analysis**

477   Our findings showed that flowering day was mainly sensitive to uncertainties (i.e. changes) in

478   photoperiod sensitivity (photop_sens) and thermal time from 'end of juvenile' to 'floral initiation'

479   (tt_end_of_juvenile) for all the three studied spring cultivars (Figure 4). The sensitivity of these

480   parameters did not only depend on the maturity habit of a cultivar, but on the location (i.e. latitude)

481   and time (i.e. sowing year; Supplementary Material Figures S3-S4). For grain yield, the ranking of

482   parameter sensitivities was the same as for flowering day for *cv* Hartog. However, uncertainties in

483   'tt_end_of_juvenile' and thermal time from 'floral initiation' to 'flowering' (tt_floral_initiation)

484   were the most influential parameters for Scout and Gregory. For all the three selected cultivars,

485   vernalisation sensitivity (vern_sens) was the least sensitive parameter for the simulated flowering

day and grain yield. Our finding stands in contrast to the findings by Zhao et al. (2014) who reported 'vern_sens' being the most sensitive parameter among the parameters influential on grain yield at two sites in eastern Australia. This can be explained by the initial ranges of parameter values that were used in that study (0-5 for 'vern_sens' and 'photop_sens'). They chose the ranges based on the range of values for existing cultivars in the APSIM cultivar-specific parameter sets, while the ranges (~0-2 for 'vern_sens' and ~2.5-4 for 'photop_sens') used in the present study were chosen based on a local calibration with the detailed phenology data and accounting for uncertainties in field observations.

In APSIM-wheat, the length of growing season, especially the vegetative and reproductive phases, determine the amount of biomass accumulation and biomass allocation to grains. Leaf area index (LAI) and dry matter biomass build up quickly until flowering. Vegetative phases are highly sensitive to photoperiod and vernalisation. The thermal time from emergence to end of juvenile is affected by photoperiod and vernalisation sensitivity factors and the number of vernalization days (Zheng et al., 2015b). This implies the importance of sowing time and maturity habit in the quantification of the sensitivity of these parameters.

Grain yield is a more complex trait than flowering day and is sensitive to numerous parameters (e.g. Zhao et al., 2014). Richter et al. (2010) ranked high the phenological development and leaf area dynamics and ranked low the physiological parameters in terms of sensitivity of grain yield to these parameters. They also showed that parameter sensitivities changed in different environments (i.e. sowing time × location). In the present study, we focused on four phenological parameters and the impact of uncertainties in those parameters on grain yield without changing other potentially influential parameters. Therefore, the estimated sensitivity may change in other studies if additional physiological and morphological parameters are included using different environments / cultivars.

4.3 Climate change impact on wheat phenology and grain yield

The present study found that wheat flowering will advance by 9 to 12 days by 2050 across the 17 selected sites in northeast Australia (Fig 10a). This is in line with findings by previous studies such as Luo (2016) who simulated 5 to 11 days advancement in the key phenological events of wheat crops by 2050. Similarly, Liu et al. (2018) suggested 7-8 days shortening of sowing-anthesis phase per degree of warming. Wang et al. (2018), Luo et al. (2018), Zheng et al. (2012) and Yang et al. (2014) also reported a substantial boost in wheat phenology under future warmer environments.

517 It is anticipated that wheat grain yield would potentially increase by 20.4-25.1% in 2050 relative to
518 2005, depending on the selected cultivar (Fig 11). These numbers must be considered the 'net'
519 impact of climate change when the optimum sowing time is chosen in each season. Our results
520 confirm the findings by Ghahramani et al. (2015), Wang et al. (2018) and Hunt et al. (2019) who
521 reported a substantial increase in wheat grain yield under future climates. For example,
522 Ghahramani et al. (2015) simulated an 18% increase in Australia's national wheat yield by 2030
523 assuming optimal adaptation. Similarly, Wang et al. (2018) adopted 1961–2000 as the baseline
524 period and reported a 10.7% increase in wheat grain yield across Australia (up to 10% in eastern
525 Australia) by 2050 under RCP 8.5, if autonomous adaptation strategies (i.e. adapted cultivated
526 cultivar and sowing time) would be adopted. Hunt et al. (2019) reported a 0.54 t/ha (~25%)
527 increase in national average wheat yield with early sowing systems combined with slower-
528 developing wheat genotypes.

529 A negative trend in water-limited yield potential (e.g. 27% between 1990 and 2015 by Hochman
530 et al., 2017) or increased effect of heat shocks have been reported on wheat yield (e.g. 4.6% in each
531 decade by Ababaei and Chenu, 2020). Yang et al. (2014) reported a generally decreasing trend in
532 NSW wheat yield (3.4 to −14.7 %) for the period centred on 2030 when compared to the baseline
533 period of 1961–1990 which is in contrast with our findings. The reason that the estimated yield
534 improvements by 2050 in the current study are higher than some of the previously reported values
535 is that we used 1990-2019 as the baseline scenario instead of 1961-2000 or 1976-2005. That is, our
536 estimates accounts for the already lower yield over the period of 1990-2019 relative to the period
537 of 1961-2000 or 1976-2005. Further, we selected the 'best' sowing date in each season, which
538 would lead to the highest grain yield under each climate scenario. Changes in wheat grain yield
539 under future climates depend on location and time of sowing as suggested by Luo (2016) and Luo
540 et al. (2018). The difference in the magnitude of increases in wheat yield between the current study
541 and Anwar et al. (2015) and the change sign opposite to some of previous studies (e.g. Yang et al.,
542 2014) could be attributed to different greenhouse gas emission scenarios, GCMs, locations, time
543 periods and cultivars considered.

4.4   Contribution of uncertainty sources

545 This study investigated the uncertainties arising from the two key sources, i.e., crop model
546 phenological parameters and climate projections. We performed analyses on the simulated values
547 of target traits as well as on the simulated impact of climate change on those traits. We showed a
548 large contribution from crop model phenological parameters to the total uncertainties in the
549 simulated flowering day and grain yield. Holzkämper et al. (2015) stated that the relative

23

550 importance of uncertainties in climate projections and model parameters depends on local
551 conditions. We can confirm this conclusion as we observed a large spatial variation in the
552 sensitivity indices across the study area.

553 On the other hand, the uncertainties in climate models are expected to play a more important role
554 than phenological parameters when the aim is to quantify the impact of climate change on target
555 traits (Figure 9). The latter is supported by Tao et al. (2018), who estimated the contribution of
556 crop parameters and GCMs to the total uncertainty in the simulated grain yield to be 42 and 46%
557 at Jokioinen and 24 and 59% at Lleida, Finland (averaged across seven crop models). Studies by
558 Challinor et al. (2009), Kassie et al. (2015) and Zhang et al. (2019) also showed climate projections
559 to be a larger contributor to the total uncertainty in simulations of the impact of climate change
560 on target traits.

561 The uncertainties in crop model structure was not addressed in the current study, though have
562 been evaluated in previous studies (Tao et al., 2009; Asseng et al., 2013; Araya et al., 2015). Some
563 studies showed that variation in crop model structures could contribute more to the total
564 uncertainty than variation across GCMs while others reported conflicting results. A recent study
565 by Liu et al. (2018) concluded that uncertainty stemming from crop model structure might be
566 larger than crop parameter estimation and the total uncertainty would be larger under a warmer
567 climate due to extra uncertainties from climate projections. These findings and conflicts suggest
568 that the contributions of crop model structure, crop parameter estimation and climate models to
569 the total uncertainty need to be evaluated at specific location(s) and with relevant crop model(s)
570 and crop(s). Moreover, continuing improvement of GCMs and using more robust calculation
571 routines for estimating crop model parameters are necessary to account for uncertainties in field
572 observations and parameter estimation procedure.

5 Conclusion

574 In this study, a slightly modified version of SUFI-2 (SUFI-2M) was used to calibrate the APSIM-
575 wheat model based on two years of experimental data at three locations in northeast Australia
576 (south-eastern Queensland). An overall RMSE of 5.5 d in simulating flowering day of 10 spring
577 wheat cultivars was found in the present study. This suggests that SUFI-2M is a robust and
578 computationally efficient calibration and uncertainty analysis algorithm which can be used for
579 similar research activities.

580 Sensitivity analyses indicated that uncertainties in photoperiod sensitivity, thermal time from 'end
581 of juvenile' to 'floral initiation' (tt_end_of_juvenile), and thermal time from 'floral initiation' to

582 'flowering' were significantly more influential than uncertainties in vernalisation sensitivity in terms

583 of simulated flowering day and grain yield. We also found a substantial inter-annual variability in

584 parameter sensitivities.

585 We estimated that climate change would advance wheat phenology by 9.5.-11.6 d at a regional

586 scale across three selected spring cultivars and would have a positive impact on wheat grain yield

587 (20.4-25.1%), if the best sowing date is selected in each season. There are high confidence in the

588 direction of the impact on the target traits, with a probability of shortened time to flowering and

589 positive impact on grain yield estimated to be 99% and 93%, respectively.

590 We found that variance decomposition of the simulated flowering day and grain yield was

591 significantly correlated with latitude. Uncertainty in the simulated flowering day and grain yield

592 was strongly influenced by the selected crop model parameters than the GCMs, which contributed

593 to the total uncertainty in the simulated values of target traits by less than 9%. On the other hand,

594 the contribution of the uncertainties from the GCMs was the largest component when the impact

595 of climate change on the target traits was to be quantified (>90% for flowering day and 49% for

596 grain yield). It was concluded that the contribution of various sources of uncertainty depended on

597 the environment (i.e. location and sowing time), the maturity habit of the cultivated cultivar, and

598 the target trait.

6 Acknowledgement

7 References

602 Ababaei, B., Chenu, K., 2020. Heat shocks increasingly impede grain filling but have little effect on grain setting across the
603 Australian wheatbelt. Agric. For. Meteorol. 284, 107889. https://doi.org/10.1016/j.agrformet.2019.107889

604 Ababaei, B., Chenu, K., 2019. Recent Trends in Drought, Heat and Frost-Induced Yield Losses Across the Australian Wheatbelt.
605 Proceedings 36, 5. https://doi.org/10.3390/proceedings2019036005

606 Ababaei, B., Najeeb, U., 2020. Detection of major weather patterns reduces number of simulations in climate impact studies. J.
607 Agron. Crop Sci. 206, 376–389. https://doi.org/10.1111/jac.12388

608 Ababaei, B., Ramezani Etedali, H., 2017. Water footprint assessment of main cereals in Iran. Agric. Water Manag. 179, 401–411.
609 https://doi.org/10.1016/j.agwat.2016.07.016

610 Ababaei, B., Sohrabi, T., Mirzaei, F., 2014. Development and application of a planning support system to assess strategies related
611 to land and water resources for adaptation to climate change. Clim. Risk Manag. 6, 39–50.
612 https://doi.org/10.1016/j.crm.2014.11.001

613 Ababaei, B., Zheng, B., Chenu, K., 2019. Impact of genotypic variations in transpiration rate on Australian wheat productivity, in:
614 Pratley, J. (Ed.), Proceedings of the 19th Australian Society of Agronomy Conference. Australian Society of Agronomy,

615   Wagga Wagga, Australia.

616   Abbaspour, K.C., 2015. SWAT-CUP: SWAT Calibration and Uncertainty Programs - A User Manual. Sci. Technol.
617   https://doi.org/10.1007/s00402-009-1032-4

618   Abbaspour, K.C., Johnson, C.A., van Genuchten, M.T., 2004. Estimating Uncertain Flow and Transport Parameters Using a
619   Sequential Uncertainty Fitting Procedure. Vadose Zo. J. 3, 1340–1352. https://doi.org/10.2136/vzj2004.1340

620   Abbaspour, K.C., Vejdani, M., Haghighat, S., Yang, J., 2007a. SWAT-CUP Calibration and Uncertainty Programs for SWAT. fourth
621   Int. SWAT Conf. 1596–1602. https://doi.org/10.1007/s00402-009-1032-4

622   Abbaspour, K.C., Yang, J., Maximov, I., Siber, R., Bogner, K., Mieleitner, J., Zobrist, J., Srinivasan, R., 2007b. Modelling hydrology
623   and water quality in the pre-alpine/alpine Thur watershed using SWAT. J. Hydrol. 333, 413–430.
624   https://doi.org/10.1016/j.jhydrol.2006.09.014

625   An-Vo, D.A., Mushtaq, S., Zheng, B., Christopher, J.T., Chapman, S.C., Chenu, K., 2018. Direct and Indirect Costs of Frost in the
626   Australian Wheatbelt. Ecol. Econ. https://doi.org/10.1016/j.ecolecon.2018.04.008

627   Andarzian, Bahram, Hoogenboom, G., Bannayan, M., Shirali, M., Andarzian, Behnam, 2015. Determining optimum sowing date
628   of wheat using CSM-CERES-Wheat model. J. Saudi Soc. Agric. Sci. https://doi.org/10.1016/j.jssas.2014.04.004

629   Anwar, M.R., Liu, D.L., Farquharson, R., Macadam, I., Abadi, A., Finlayson, J., Wang, B., Ramilan, T., 2015. Climate change impacts
630   on phenology and yields of five broadacre crops at four climatologically distinct locations in Australia. Agric. Syst. 132, 133–
631   144. https://doi.org/10.1016/j.agsy.2014.09.010

632   Araya, A., Hoogenboom, G., Luedeling, E., Hadgu, K.M., Kisekka, I., Martorano, L.G., 2015. Assessment of maize growth and
633   yield using crop models under present and future climate in southwestern Ethiopia. Agric. For. Meteorol. 214–215, 252–
634   265. https://doi.org/10.1016/j.agrformet.2015.08.259

635   Asseng, S., Ewert, F., Martre, P., Rötter, R.P., Lobell, D.B., Cammarano, D., Kimball, B.A., Ottman, M.J., Wall, G.W., White, J.W.,
636   Reynolds, M.P., Alderman, P.D., Prasad, P.V.V., Aggarwal, P.K., Anothai, J., Basso, B., Biernath, C., Challinor, A.J., De
637   Sanctis, G., Doltra, J., Fereres, E., Garcia-Vila, M., Gayler, S., Hoogenboom, G., Hunt, L.A., Izaurralde, R.C., Jabloun, M.,
638   Jones, C.D., Kersebaum, K.C., Koehler, A.K., Müller, C., Naresh Kumar, S., Nendel, C., O'leary, G., Olesen, J.E., Palosuo,
639   T., Priesack, E., Eyshi Rezaei, E., Ruane, A.C., Semenov, M.A., Shcherbak, I., Stöckle, C., Stratonovitch, P., Streck, T., Supit,
640   I., Tao, F., Thorburn, P.J., Waha, K., Wang, E., Wallach, D., Wolf, J., Zhao, Z., Zhu, Y., 2015. Rising temperatures reduce
641   global wheat production. Nat. Clim. Chang. 5, 143–147. https://doi.org/10.1038/nclimate2470

642   Asseng, S., Ewert, F., Rosenzweig, C., Jones, J.W., Hatfield, J.L., Ruane, A.C., Boote, K.J., Thorburn, P.J., Rötter, R.P., Cammarano,
643   D., Brisson, N., Basso, B., Martre, P., Aggarwal, P.K., Angulo, C., Bertuzzi, P., Biernath, C., Challinor, A.J., Doltra, J., Gayler,
644   S., Goldberg, R., Grant, R., Heng, L., Hooker, J., Hunt, L.A., Ingwersen, J., Izaurralde, R.C., Kersebaum, K.C., Müller, C.,
645   Naresh Kumar, S., Nendel, C., O'Leary, G., Olesen, J.E., Osborne, T.M., Palosuo, T., Priesack, E., Ripoche, D., Semenov,
646   M.A., Shcherbak, I., Steduto, P., Stöckle, C., Stratonovitch, P., Streck, T., Supit, I., Tao, F., Travasso, M., Waha, K., Wallach,
647   D., White, J.W., Williams, J.R., Wolf, J., 2013. Uncertainty in simulating wheat yields under climate change. Nat. Clim. Chang.
648   3, 627–632. https://doi.org/10.1038/ncliamte1916

649   Asseng, S., Jamieson, P.. D., Kimball, B., Pinter, P., Sayre, K., Bowden, J.. W., Howden, S.. M., 2004. Simulated wheat growth
650   affected by rising temperature, increased water deficit and elevated atmospheric CO2. F. Crop. Res. 85, 85–102.
651   https://doi.org/10.1016/S0378-4290(03)00154-0

652   Asseng, S., Turner, N.C., Keating, B.A., 2001. Analysis of water- and nitrogen-use efficiency of wheat in a Mediterranean climate.
653   Plant Soil 233, 127–143. https://doi.org/10.1023/A:1010381602223

654   Bert, F.E., Laciana, C.E., Podestá, G.P., Satorre, E.H., Menéndez, A.N., 2007. Sensitivity of CERES-Maize simulated yields to
655   uncertainty in soil properties and daily solar radiation. Agric. Syst. 94, 141–150. https://doi.org/10.1016/j.agsy.2006.08.003

656   Brennan, P.S., Martin, D.J., Eisemann, R.L., Mason, L.R., Sheppard, J.A., Norris, R.G., Smith, G.D., Uebergang, R.W., The, D.,
657   Keys, P.J., Mackay, M.C., 1991. Register of australian winter cereal cultivars: Triticum aestivum ssp. vulgare (bread wheat)

658   cv. janz. Aust. J. Exp. Agric. 31, 727. https://doi.org/10.1071/EA9910727

659 Brill, R., Gardner, M., Graham, R., Fettell, N., 2013. Will low protein become the new norm?, GRDC Update Papers. Grains
660   Research and Development Corporation.

661 Challinor, A.J., Smith, M.S., Thornton, P., 2013. Use of agro-climate ensembles for quantifying uncertainty and informing
662   adaptation. Agric. For. Meteorol. https://doi.org/10.1016/j.agrformet.2012.09.007

663 Challinor, A.J., Wheeler, T., Hemming, D., Upadhyaya, H.D., 2009a. Ensemble yield simulations: Crop and climate uncertainties,
664   sensitivity to temperature and genotypic adaptation to climate change. Clim. Res. 38, 117–127.
665   https://doi.org/10.3354/cr00779

666 Challinor, A.J., Wheeler, T., Hemming, D., Upadhyaya, H.D., 2009b. Ensemble yield simulations: Crop and climate uncertainties,
667   sensitivity to temperature and genotypic adaptation to climate change. Clim. Res. 38, 117–127.
668   https://doi.org/10.3354/cr00779

669 Chenu, K., Cooper, M., Hammer, G.L., Mathews, K.L., Dreccer, M.F., Chapman, S.C., 2011. Environment characterization as an
670   aid to wheat improvement: Interpreting genotype-environment interactions by modelling water-deficit patterns in North-
671   Eastern Australia. J. Exp. Bot. 62, 1743–1755. https://doi.org/10.1093/jxb/erq459

672 Chenu, K., Deihimfard, R., Chapman, S.C., 2013. Large-scale characterization of drought pattern: A continent-wide modelling
673   approach applied to the Australian wheatbelt - spatial and temporal trends. New Phytol. https://doi.org/10.1111/nph.12192

674 Christopher, J.T., Christopher, M.J., Borrell, A.K., Fletcher, S., Chenu, K., 2016. Stay-green traits to improve wheat adaptation in
675   well-watered and water-limited environments. J. Exp. Bot. https://doi.org/10.1093/jxb/erw276

676 Christopher, J.T., Manschadi, A.M., Hammer, G.L., Borrell, A.K., 2008. Developmental and physiological traits associated with
677   high yield and stay-green phenotype in wheat. Aust. J. Agric. Res. 59, 354–364. https://doi.org/10.1071/AR07193

678 Condon, A.G., Richards, R.A., Rebetzke, G.J., Farquhar, G.D., Tausz-Posch, S., Seneweera, S., Norton, R.M., Fitzgerald, G.J.,
679   Tausz, M., 2012. Can a wheat cultivar with high transpiration efficiency maintain its yield advantage over a near-isogenic
680   cultivar under elevated CO_2? F. Crop. Res. https://doi.org/10.1093/jxb/erh277

681 DeJonge, K.C., Ascough, J.C., Ahmadi, M., Andales, A.A., Arabi, M., 2012. Global sensitivity and uncertainty analysis of a dynamic
682   agroecosystem model under different irrigation treatments. Ecol. Modell. 231, 113–125.
683   https://doi.org/10.1016/j.ecolmodel.2012.01.024

684 Faramarzi, M., Yang, H., Schulin, R., Abbaspour, K.C., 2010. Modeling wheat yield and crop water productivity in Iran: Implications
685   of agricultural water management for wheat production. Agric. Water Manag. 97, 1861–1875.
686   https://doi.org/10.1016/j.agwat.2010.07.002

687 Flohr, B.M., Hunt, J.R., Kirkegaard, J.A., Evans, J.R., 2017. Water and temperature stress define the optimal flowering period for
688   wheat in south-eastern Australia. F. Crop. Res. 209, 108–119. https://doi.org/10.1016/j.fcr.2017.04.012

689 Gao, Y., Wallach, D., Liu, B., Dingkuhn, M., Boote, K.J., Singh, U., Asseng, S., Kahveci, T., He, J., Zhang, R., Confalonieri, R.,
690   Hoogenboom, G., 2020. Comparison of three calibration methods for modeling rice phenology. Agric. For. Meteorol. 280.
691   https://doi.org/10.1016/j.agrformet.2019.107785

692 Ghahramani, A., Kokic, P.N., Moore, A.D., Zheng, B., Chapman, S.C., Howden, M.S., Crimp, S.J., 2015. The value of adapting to
693   climate change in Australian wheat farm systems: farm to cross-regional scale. Agric. Ecosyst. Environ. 211, 112–125.
694   https://doi.org/10.1016/j.agee.2015.05.011

695 Graham, R., Peter, Martin, Greg, B., Peter, Matthews, McMullen, G., 2015. Wheat Variety Response To Sowing Time. Tamworth.

696 Hammer, G.L., McLean, G., Chapman, S., Zheng, B., Doherty, A., Harrison, M.T., Van Oosterom, E., Jordan, D., 2014. Crop
697   design for specific adaptation in variable dryland production environments. Crop Pasture Sci. 65, 614–626.
698   https://doi.org/10.1071/CP14088

699 Hochman, Z., Gobbett, D.L., Horan, H., 2017. Climate trends account for stalled wheat yields in Australia since 1990. Glob. Chang.

700   Biol. 23, 2071–2081. https://doi.org/10.1111/gcb.13604

701   Hochman, Z., Holzworth, D., Hunt, J.R., 2009. Potential to improve on-farm wheat yield and WUE in Australia. Crop Pasture Sci.
702   60, 708–716. https://doi.org/10.1071/CP09064

703   Holzkämper, A., Klein, T., Seppelt, R., Fuhrer, J., 2015. Assessing the propagation of uncertainties in multi-objective optimization
704   for   agro-ecosystem   adaptation   to   climate   change.   Environ.   Model.   Softw.   66,   27–35.
705   https://doi.org/10.1016/j.envsoft.2014.12.012

706   Holzworth, D.P., Huth, N.I., DeVoil, P.G., Zurcher, E.J., Herrmann, N.I., McLean, G., Chenu, K., van Oosterom, E.J., Snow, V.,
707   Murphy, C., Moore, A.D., Brown, H., Whish, J.P.M., Verrall, S., Fainges, J., Bell, L.W., Peake, A.S., Poulton, P.L., Hochman,
708   Z., Thorburn, P.J., Gaydon, D.S., Dalgliesh, N.P., Rodriguez, D., Cox, H., Chapman, S., Doherty, A., Teixeira, E., Sharp, J.,
709   Cichota, R., Vogeler, I., Li, F.Y., Wang, E., Hammer, G.L., Robertson, M.J., Dimes, J.P., Whitbread, A.M., Hunt, J., van
710   Rees, H., McClelland, T., Carberry, P.S., Hargreaves, J.N.G., MacLeod, N., McDonald, C., Harsdorf, J., Wedgwood, S.,
711   Keating, B.A., 2014. APSIM – Evolution towards a new generation of agricultural systems simulation. Environ. Model.
712   Softw. 62, 327–350. https://doi.org/10.1016/j.envsoft.2014.07.009

713   Hunt, J.R., Lilley, J.M., Trevaskis, B., Flohr, B.M., Peake, A., Fletcher, A., Zwart, A.B., Gobbett, D., Kirkegaard, J.A., 2019. Early
714   sowing systems can boost Australian wheat yields despite recent climate change. Nat. Clim. Chang.
715   https://doi.org/10.1038/s41558-019-0417-9

716   Hussain, J., Khaliq, T., Ahmad, A., Akhtar, J., 2018. Performance of four crop model for simulations of wheat phenology, leaf
717   growth, biomass and yield across planting dates. PLoS One. https://doi.org/10.1371/journal.pone.0197546

718   Iizumi, T., Yokozawa, M., Nishimori, M., 2009. Parameter estimation and uncertainty analysis of a large-scale crop model for paddy
719   rice: Application   of   a   Bayesian   approach.   Agric.   For.   Meteorol.   149,   333–348.
720   https://doi.org/10.1016/j.agrformet.2008.08.015

721   Jeffrey, S.J., Carter, J.O., Moodie, K.B., Beswick, A.R., 2001. Using spatial interpolation to construct a comprehensive archive of
722   Australian climate data. Environ. Model. Softw. 16, 309–330. https://doi.org/10.1016/S1364-8152(01)00008-1

723   Kassie, B.T., Asseng, S., Rotter, R.P., Hengsdijk, H., Ruane, A.C., Van Ittersum, M.K., 2015. Exploring climate change impacts
724   and adaptation options for maize production in the Central Rift Valley of Ethiopia using different climate change scenarios
725   and crop models. Clim. Change 129, 145–158. https://doi.org/10.1007/s10584-014-1322-x

726   Keating, B.A., Carberry, P.., Hammer, G.., Probert, M.., Robertson, M.., Holzworth, D., Huth, N.., Hargreaves, J.N.., Meinke, H.,
727   Hochman, Z., McLean, G., Verburg, K., Snow, V., Dimes, J.., Silburn, M., Wang, E., Brown, S., Bristow, K.., Asseng, S.,
728   Chapman, S., McCown, R.., Freebairn, D.., Smith, C.., 2003. An overview of APSIM, a model designed for farming systems
729   simulation. Eur. J. Agron. 18, 267–288. https://doi.org/10.1016/S1161-0301(02)00108-9

730   Kumar, R., Shankar, V., Jat, M.K., 2014. Sensitivity Analysis of Nonlinear Model Parameters in a Multilayer Root Zone. J. Hydrol.
731   Eng. 19, 462–471. https://doi.org/10.1061/(ASCE)HE.1943-5584.0000804

732   Lilley, J.M., Kirkegaard, J.A., 2007. Seasonal variation in the value of subsoil water to wheat: Simulation studies in southern New
733   South Wales. Aust. J. Agric. Res. 58, 1115–1128. https://doi.org/10.1071/AR07046

734   Liu, B., Martre, P., Ewert, F., Porter, J.R., Challinor, A.J., Müller, C., Ruane, A.C., Waha, K., Thorburn, P.J., Aggarwal, P.K., Ahmed,
735   M., Balkovič, J., Basso, B., Biernath, C., Bindi, M., Cammarano, D., De Sanctis, G., Dumont, B., Espadafor, M., Eyshi
736   Rezaei, E., Ferrise, R., Garcia-Vila, M., Gayler, S., Gao, Y., Horan, H., Hoogenboom, G., Izaurralde, R.C., Jones, C.D.,
737   Kassie, B.T., Kersebaum, K.C., Klein, C., Koehler, A., Maiorano, A., Minoli, S., Montesino San Martin, M., Naresh Kumar,
738   S., Nendel, C., O'Leary, G.J., Palosuo, T., Priesack, E., Ripoche, D., Rötter, R.P., Semenov, M.A., Stöckle, C., Streck, T.,
739   Supit, I., Tao, F., Van der Velde, M., Wallach, D., Wang, E., Webber, H., Wolf, J., Xiao, L., Zhang, Z., Zhao, Z., Zhu, Y.,
740   Asseng, S., 2019. Global wheat production with 1.5 and 2.0°C above pre-industrial warming. Glob. Chang. Biol. 25, 1428–
741   1444. https://doi.org/10.1111/gcb.14542

742   Liu, K., Harrison, M.T., Hunt, J., Angessa, T.T., Meinke, H., Li, C., Tian, X., Zhou, M., 2020. Identifying optimal sowing and

743   flowering periods for barley in Australia: a modelling approach. Agric. For. Meteorol. 282–283.
744   https://doi.org/10.1016/j.agrformet.2019.107871

745   Liu, L., Wallach, D., Li, J., Liu, B., Zhang, L., Tang, L., Zhang, Y., Qiu, X., Cao, W., Zhu, Y., 2018. Uncertainty in wheat phenology
746   simulation induced by cultivar parameterization under climate warming. Eur. J. Agron. 94, 46–53.
747   https://doi.org/10.1016/j.eja.2017.12.001

748   Lobell, D.B., Hammer, G.L., Chenu, K., Zheng, B., McLean, G., Chapman, S.C., 2015. The shifting influence of drought and heat
749   stress for crops in northeast Australia. Glob. Chang. Biol. 21, 4115–4127. https://doi.org/10.1111/gcb.13022

750   Luo, Q., 2016. Performance of agro-climate indices and wheat grain yield in a changing climate. Clim. Res. 69, 143–154.
751   https://doi.org/10.3354/cr01400

752   Luo, Q., Jones, R.N., Williams, M., Bryan, B., Bellotti, W., 2005. Probabilistic distributions of regional climate change and their
753   application in risk analysis of wheat production. Clim. Res. https://doi.org/10.3354/cr029041

754   Luo, Q., O'Leary, G., Cleverly, J., Eamus, D., 2018. Effectiveness of time of sowing and cultivar choice for managing climate
755   change: wheat crop phenology and water use efficiency. Int. J. Biometeorol. 62, 1049–1061.
756   https://doi.org/10.1007/s00484-018-1508-4

757   McKay, M.D., Beckman, R.J., Conover, W.J., 1979. A Comparison of Three Methods for Selecting Values of Input Variables in
758   the Analysis of Output from a Computer Code. Technometrics 21, 239. https://doi.org/10.2307/1268522

759   Pogson, M., Hastings, A., Smith, P., 2012. Sensitivity of crop model predictions to entire meteorological and soil input datasets
760   highlights vulnerability to drought. Environ. Model. Softw. https://doi.org/10.1016/j.envsoft.2011.10.008

761   Pörtner, H.-O., Karl, D., Boyd, P.W., Cheung, W., Lluch- Cota, S.E., Nojiri, Y., Schmidt, D., Zavialov, P., 2014. Ocean sytems, in:
762   Climate Change 2014: Impacts, Adaptation, and Vulnerability. Part A: Global and Sectoral Aspects. Contribution of Working
763   Group II to the Fifth Assessment Report of the Intergovernmental Panel of Climate Change.

764   Press, W.H., Flannery, B.P., Teukolsky, S. a., Vetterling, W.T., 1992. The Art of Scientific Computing. Numer. Recipes.

765   R Core Team, 2017. R: A Language and Environment for Statistical Computing, R Foundation for Statistical Computing. Vienna,
766   Austria. https://www.r-project.org.

767   Reyenga, P.J., Howden, S.M., Meinke, H., McKeon, G.M., 1999. Modelling global change impacts on wheat cropping in south-east
768   Queensland, Australia. Environ. Model. Softw. 14, 297–306. https://doi.org/10.1016/S1364-8152(98)00081-4

769   Richter, G.M., Acutis, M., Trevisiol, P., Latiri, K., Confalonieri, R., 2010. Sensitivity analysis for a complex crop model applied to
770   Durum wheat in the Mediterranean. Eur. J. Agron. 32, 127–136. https://doi.org/10.1016/j.eja.2009.09.002

771   Rosenzweig, C., Elliott, J., Deryng, D., Ruane, A.C., Müller, C., Arneth, A., Boote, K.J., Folberth, C., Glotter, M., Khabarov, N.,
772   Neumann, K., Piontek, F., Pugh, T.A.M., Schmid, E., Stehfest, E., Yang, H., Jones, J.W., 2014. Assessing agricultural risks
773   of climate change in the 21st century in a global gridded crop model intercomparison. Proc. Natl. Acad. Sci. U. S. A.
774   https://doi.org/10.1073/pnas.1222463110

775   Saltelli, A., Ratto, M., Andres, T., Campolongo, F., Cariboni, J., Gatelli, D., Saisana, M., Tarantola, S., 2008. Global Sensitivity
776   Analysis. The Primer, Global Sensitivity Analysis. The Primer. https://doi.org/10.1002/9780470725184

777   Seidel, S.J., Palosuo, T., Thorburn, P., Wallach, D., 2018. Towards improved calibration of crop models – Where are we now and
778   where should we go? Eur. J. Agron. https://doi.org/10.1016/j.eja.2018.01.006

779   Stöckle, C., Balkovič, J., Horan, H., Thorburn, P.J., Waha, K., Stratonovitch, P., O'Leary, G.J., Maiorano, A., Wang, E., Ewert, F.,
780   Gayler, S., Zhang, Z., Ruane, A.C., Klein, C., Basso, B., Reynolds, M.P., Tao, F., Nendel, C., Ferrise, R., Koehler, A.,
781   Montesino San Martin, M., Ripoche, D., Semenov, M.A., Naresh Kumar, S., Babar, M.A., Wolf, J., Asseng, S., Olesen, J.E.,
782   Minoli, S., Izaurralde, R.C., Girousse, C., Müller, C., Garcia-Vila, M., Rötter, R.P., Liu, B., Webber, H., Zhao, Z., Kassie,
783   B.T., Wallach, D., Porter, J.R., Kheir, A.M.S., Xiao, L., Biernath, C., Jones, C.D., Dumont, B., Gao, Y., Motzo, R.,
784   Cammarano, D., Bindi, M., Jabloun, M., Aggarwal, P.K., Supit, I., Eyshi Rezaei, E., Giunta, F., Priesack, E., Martre, P.,
785   Kersebaum, K.-C., Hoogenboom, G., Zhu, Y., Streck, T., Fereres, E., Ahmed, M., Palosuo, T., De Sanctis, G., Van der

29

786 Velde, M., Fitzgerald, G.J., Challinor, A.J., 2018. Climate change impact and adaptation for wheat protein. Glob. Chang.
787   Biol. 25, 155–173. https://doi.org/10.1111/gcb.14481

788 Tao, F., Hayashi, Y., Zhang, Z., Sakamoto, T., Yokozawa, M., 2008. Global warming, rice production, and water use in China:
789   Developing a probabilistic assessment. Agric. For. Meteorol. https://doi.org/10.1016/j.agrformet.2007.09.012

790 Tao, F., Rötter, R.P., Palosuo, T., Gregorio Hernández Díaz-Ambrona, C., Mínguez, M.I., Semenov, M.A., Kersebaum, K.C.,
791   Nendel, C., Specka, X., Hoffmann, H., Ewert, F., Dambreville, A., Martre, P., Rodríguez, L., Ruiz-Ramos, M., Gaiser, T.,
792   Höhn, J.G., Salo, T., Ferrise, R., Bindi, M., Cammarano, D., Schulman, A.H., Gregorio Hernández Díaz-Ambrona, C.,
793   Mínguez, M.I., Semenov, M.A., Kersebaum, K.C., Nendel, C., Specka, X., Hoffmann, H., Ewert, F., Dambreville, A., Martre,
794   P., Rodríguez, L., Ruiz-Ramos, M., Gaiser, T., Höhn, J.G., Salo, T., Ferrise, R., Bindi, M., Cammarano, D., Schulman, A.H.,
795   2018. Contribution of crop model structure, parameters and climate projections to uncertainty in climate change impact
796   assessments. Glob. Chang. Biol. 24, 1291–1307. https://doi.org/10.1111/gcb.14019

797 Tao, F., Yokozawa, M., Zhang, Z., 2009. Modelling the impacts of weather and climate variability on crop productivity over a large
798   area: A new process-based model development, optimization, and uncertainties analysis. Agric. For. Meteorol. 149, 831–
799   850. https://doi.org/10.1016/j.agrformet.2008.11.004

800 Tausz-Posch, S., Seneweera, S., Norton, R.M., Fitzgerald, G.J., Tausz, M., 2012. Can a wheat cultivar with high transpiration
801   efficiency maintain its yield advantage over a near-isogenic cultivar under elevated CO2? F. Crop. Res. 133, 160–166.
802   https://doi.org/10.1016/j.fcr.2012.04.007

803 Taylor, K.E., Stouffer, R.J., Meehl, G.A., 2012. An Overview of CMIP5 and the Experiment Design. Bull. Am. Meteorol. Soc. 93,
804   485–498. https://doi.org/10.1175/BAMS-D-11-00094.1

805 Wallach, D., Thorburn, P.J., 2017. Estimating uncertainty in crop model predictions: Current situation and future prospects. Eur.
806   J. Agron. 88, A1–A7. https://doi.org/10.1016/j.eja.2017.06.001

807 Wang, B., Liu, D.L., O'Leary, G.J., Asseng, S., Macadam, I., Lines-Kelly, R., Yang, X., Clark, A., Crean, J., Sides, T., Xing, H., Mi,
808   C., Yu, Q., 2018. Australian wheat production expected to decrease by the late 21st century. Glob. Chang. Biol. 24, 2403–
809   2415. https://doi.org/10.1111/gcb.14034

810 Wang, E., Martre, P., Zhao, Z., Ewert, F., Maiorano, A., Rötter, R.P., Kimball, B.A., Ottman, M.J., Wall, G.W., White, J.W.,
811   Reynolds, M.P., Alderman, P.D., Aggarwal, P.K., Anothai, J., Basso, B., Biernath, C., Cammarano, D., Challinor, A.J., De
812   Sanctis, G., Doltra, J., Fereres, E., Garcia-Vila, M., Gayler, S., Hoogenboom, G., Hunt, L.A., Izaurralde, R.C., Jabloun, M.,
813   Jones, C.D., Kersebaum, K.C., Koehler, A.K., Liu, L., Müller, C., Naresh Kumar, S., Nendel, C., O'Leary, G., Olesen, J.E.,
814   Palosuo, T., Priesack, E., Eyshi Rezaei, E., Ripoche, D., Ruane, A.C., Semenov, M.A., Shcherbak, I., Stöckle, C.,
815   Stratonovitch, P., Streck, T., Supit, I., Tao, F., Thorburn, P., Waha, K., Wallach, D., Wang, Z., Wolf, J., Zhu, Y., Asseng, S.,
816   2017. The uncertainty of crop yield projections is reduced by improved temperature response functions. Nat. Plants 3.
817   https://doi.org/10.1038/nplants.2017.102

818 Webber, H., Olesen, J.E., Müller, C., Fronzek, S., Ruane, A., Bourgault, M., Martre, P., Others, Wallach, D., 2018. Diverging
819   importance of drought stress for maize and winter wheat in Europe. Nat. Commun. in press, 4249.
820   https://doi.org/10.1038/s41467-018-06525-2

821 White, J.W., Hoogenboom, G., Kimball, B.A., Wall, G.W., 2011. Methodologies for simulating impacts of climate change on crop
822   production. F. Crop. Res. https://doi.org/10.1016/j.fcr.2011.07.001

823 Yang, Yanmin, Liu, D.L., Anwar, M.R., Zuo, H., Yang, Yonghui, 2014. Impact of future climate change on wheat production in
824   relation to plant-available water capacity in a semiaridenvironment. Theor. Appl. Climatol. https://doi.org/10.1007/s00704-
825   013-0895-z

826 Yuan, S., Peng, S., Li, T., 2017. Evaluation and application of the ORYZA rice model under different crop managements with
827   high-yielding rice cultivars in central China. F. Crop. Res. https://doi.org/10.1016/j.fcr.2017.07.010

828 Zadoks, J.C., Chang, T.T., Konzak, C.F., 1974. A decimal code for the growth stages of cereals. Weed Res. 14, 415–421.

829   https://doi.org/10.1111/j.1365-3180.1974.tb01084.x

830 Zhang, Y., Zhao, Y., Feng, L., 2019. Higher contributions of uncertainty from global climate models than crop models in maize-
831   yield simulations under climate change. Meteorol. Appl. 26, 74–82. https://doi.org/10.1002/met.1738

832 Zhao, G., Bryan, B.A., Song, X., 2014. Sensitivity and uncertainty analysis of the APSIM-wheat model: Interactions between
833   cultivar, environmental, and management parameters. Ecol. Modell. 279, 1–11.
834   https://doi.org/10.1016/j.ecolmodel.2014.02.003

835 Zheng, B., Chapman, S.C., Christopher, J.T., Frederiks, T.M., Chenu, K., 2015a. Frost trends and their estimated impact on yield
836   in the Australian wheatbelt. J. Exp. Bot. 66, 3611–3623. https://doi.org/10.1093/jxb/erv163

837 Zheng, B., Chenu, K., Chapman, S.C., 2016. Velocity of temperature and flowering time in wheat - assisting breeders to keep pace
838   with climate change. Glob. Chang. Biol. 22, 921–933. https://doi.org/10.1111/gcb.13118

839 Zheng, B., Chenu, K., Doherty, A., Chapman, S., 2015b. The APSIM-Wheat Module (7.5 R3008).

840 Zheng, B., Chenu, K., Fernanda Dreccer, M., Chapman, S.C., 2012. Breeding for the future: what are the potential impacts of
841   future frost and heat events on sowing and flowering time requirements for Australian bread wheat (*Triticum aestivium*)
842   varieties? Glob. Chang. Biol. 18, 2899–2914. https://doi.org/10.1111/j.1365-2486.2012.02724.x

843 Zheng, Z., Kilian, A., Yan, G., Liu, C., 2014. QTL conferring fusarium crown rot resistance in the elite bread wheat variety EGA
844   Wylie. PLoS One 9, e96011. https://doi.org/10.1371/journal.pone.0096011

845 Ziehn, T., Law, R.M., Rayner, P.J., Roff, G., 2016. Designing optimal greenhouse gas monitoring networks for Australia. Geosci.
846   Instrumentation, Methods Data Syst. 5, 1–15. https://doi.org/10.5194/gi-5-1-2016

847

848